Physica D 239 (2010) 1968–1983

Contents lists available at ScienceDirect

Physica D

journal homepage: www.elsevier.com/locate/physd

Singular standing-ring solutions of nonlinear partial differential equations

Guy Baruch, Gadi Fibich *, Nir Gavish

School of Mathematical Sciences, Tel Aviv University, Tel Aviv 69978, Israel

ARTICLE INFO

Article history:
Received 10 July 2009
Received in revised form
21 July 2010
Accepted 22 July 2010
Available online 27 July 2010
Communicated by J. Bronski

Keywords:
Nonlinear Schrödinger equation
Biharmonic nonlinear Schrödinger equation
Nonlinear heat equation
Biharmonic nonlinear heat equation
Blowup
Ring

ABSTRACT

We present a general framework for constructing singular solutions of nonlinear evolution equations that become singular on a d-dimensional sphere, where $d > 1$. The asymptotic profile and blowup rate of these solutions are the same as those of solutions of the corresponding one-dimensional equation that become singular at a point. We provide a detailed numerical investigation of these new singular solutions for the following equations: The nonlinear Schrödinger equation $i\psi_t(t,\mathbf{x}) + \Delta\psi + |\psi|^{2\sigma}\psi = 0$ with $\sigma > 2$, the biharmonic nonlinear Schrödinger equation $i\psi_t(t,\mathbf{x}) - \Delta^2\psi + |\psi|^{2\sigma}\psi = 0$ with $\sigma > 4$, the nonlinear heat equation $\psi_t(t,\mathbf{x}) - \Delta\psi - |\psi|^{2\sigma}\psi = 0$ with $\sigma > 0$, and the nonlinear biharmonic heat equation $\psi_t(t,\mathbf{x}) + \Delta^2\psi - |\psi|^{2\sigma}\psi = 0$ with $\sigma > 0$.

1. Introduction

In this study, we consider nonlinear evolution equations of the form

$$u_t(t,\mathbf{x}) = F[u, \Delta u, \Delta^2 u, \ldots], \quad \mathbf{x} \in \mathbb{R}^d, \ d > 1. \tag{1}$$

Examples for such equations are the nonlinear Schrödinger equation, the biharmonic nonlinear Schrödinger equation, the nonlinear heat equation, and the biharmonic nonlinear heat equation. It is well known that these equations admit solutions that become singular at a point. Recently, it was discovered that the nonlinear Schrödinger equation with a quintic nonlinearity admits solutions that become singular on a d-dimensional sphere [1–4], see Fig. 1. Following [2], we refer to these solutions as *singular standing-ring* solutions.

The main goal of this study is to present a general framework for constructing singular standing-ring solutions of nonlinear evolution equations of the form (1). In order to understand the basic idea, let us assume that Eq. (1) admits a singular standing-ring solution. Then, near the singularity, Eq. (1) reduces to the one-dimensional equation

$$u_t(t,r) = F[u, u_{rr}, u_{rrrr}, \ldots], \quad r = |\mathbf{x}|. \tag{2}$$

Hence, Eq. (2) "should" admit a solution that becomes singular at a point. Conversely, if the one-dimensional equation (2) admits a solution that becomes singular at a point, then Eq. (1) "should" admit a standing-ring singular solution. Moreover, the asymptotic profile and blowup rate of the standing-ring solutions of (1) "should" be the same as those of the corresponding solution of the one-dimensional equation (2).

The above argument is obviously very informal. Nevertheless, in what follows we will provide numerical evidence in support of the relation between standing-ring singular solutions of (1) and singular solutions of the one-dimensional equation (2).

1.1. Peak-type and ring-type singular solutions of the nonlinear Schrödinger equation (NLS)—review

The focusing nonlinear Schrödinger equation (NLS)

$$i\psi_t(t,\mathbf{x}) + \Delta\psi + |\psi|^{2\sigma}\psi = 0, \qquad \psi(0,\mathbf{x}) = \psi_0(\mathbf{x}), \tag{3}$$

where $\mathbf{x} \in \mathbb{R}^d$ and $\Delta = \partial_{x_1x_1} + \cdots + \partial_{x_dx_d}$, is one of the canonical nonlinear equations in physics, arising in various fields such as nonlinear optics, plasma physics, Bose–Einstein condensates, and surface waves. One of the important properties of the NLS is that it admits solutions which become singular at a finite time, i.e.,

$$\lim_{t\to T_c} \|\psi\|_{H^1} = \infty, \quad 0 < T_c < \infty.$$

The NLS is called *subcritical* if $\sigma d < 2$. In this case, all solutions exist globally. In contrast, solutions of the *critical* ($\sigma d = 2$) and *supercritical* ($\sigma d > 2$) NLS can become singular in finite time.

* Corresponding author.
E-mail addresses: guy.baruch@math.tau.ac.il (G. Baruch), fibich@tau.ac.il, fibich@math.tau.ac.il (G. Fibich), nirgvsh@tau.ac.il (N. Gavish).

0167-2789/$ – see front matter © 2010 Elsevier B.V. All rights reserved.
doi:10.1016/j.physd.2010.07.009

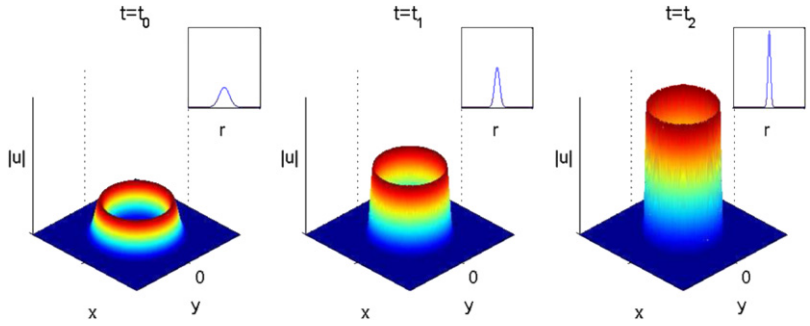

Fig. 1. Illustration of a two-dimensional singular standing-ring solution at times $t_0 < t_1 < t_2$. The insets show the radial profile of u.

When the initial condition ψ_0 is radially-symmetric, Eq. (3) reduces to

$$\begin{aligned} &i\psi_t(t,r) + \psi_{rr} + \frac{d-1}{r}\psi_r + |\psi|^{2\sigma}\psi = 0, \\ &\psi(0,r) = \psi_0(r), \quad d > 1, \end{aligned} \tag{4}$$

where $r = |\mathbf{x}|$. Let us denote the location of the maximal amplitude by

$$r_{\max}(t) = \arg\max_r |\psi|.$$

Singular solutions of (4) are called '*peak-type*' when $r_{\max}(t) \equiv 0$ for $0 \le t \le T_c$, and '*ring-type*' when $r_{\max}(t) > 0$ for $0 \le t < T_c$.

Until a few years ago, the only known singular NLS solutions were peak-type. In the critical case $\sigma d = 2$, it has been rigorously shown [5] that peak-type solutions are self-similar near the singularity, i.e., $\psi \sim \psi_R$, where

$$\psi_R(t,r) = \frac{1}{L^{1/\sigma}(t)} R(\rho)\, e^{i\tau + i\frac{L_t}{4L}r^2},$$

$$\tau = \int_0^t \frac{ds}{L^2(s)}, \qquad \rho = \frac{r - r_{\max}(t)}{L(t)}, \quad r_{\max}(t) \equiv 0,$$

the self-similar profile $R(\rho)$ attains its global maximum at $\rho = 0$, and the blowup rate $L(t)$ is given by the *loglog law*

$$L(t) \sim \left(\frac{2\pi(T_c - t)}{\log\log 1/(T_c - t)}\right)^{\frac{1}{2}}, \quad t \to T_c. \tag{5}$$

In the supercritical case ($\sigma d > 2$), the rigorous theory is far less developed. However, formal calculations and numerical simulations [6] suggest that peak-type solutions of the supercritical NLS collapse with the self-similar ψ_S profile, i.e., $\psi \sim \psi_S$, where

$$\psi_S(t,r) = \frac{1}{L^{1/\sigma}(t)} S(\rho)\, e^{i\tau}, \tag{6a}$$

$$\tau = \int_0^t \frac{ds}{L^2(s)}, \qquad \rho = \frac{r - r_{\max}(t)}{L(t)}, \quad r_{\max}(t) \equiv 0, \tag{6b}$$

$|S(\rho)|$ attains its global maximum at $\rho = 0$, and the blowup rate is a square-root, i.e.,

$$L(t) \sim \kappa\sqrt{T_c - t}, \quad t \to T_c. \tag{6c}$$

In the last few years, new singular solutions of the NLS were discovered, which are ring-type [7,2,1,4,3]. In [2], we showed that the NLS with $d > 1$ and $\frac{2}{d} \le \sigma \le 2$ admits singular ring-type solutions that collapse with the ψ_Q profile, i.e., $\psi \sim \psi_Q$, where

$$\psi_Q(t,r) = \frac{1}{L^{1/\sigma}(t)} Q(\rho)\, e^{i\tau + i\alpha\frac{L_t}{4L}r^2 + i(1-\alpha)\frac{L_t}{4L}(r - r_{\max}(t))^2}, \tag{7a}$$

$$\tau = \int_0^t \frac{ds}{L^2(s)}, \qquad \rho = \frac{r - r_{\max}(t)}{L(t)}, \quad r_{\max}(t) = r_0 L^\alpha(t), \tag{7b}$$

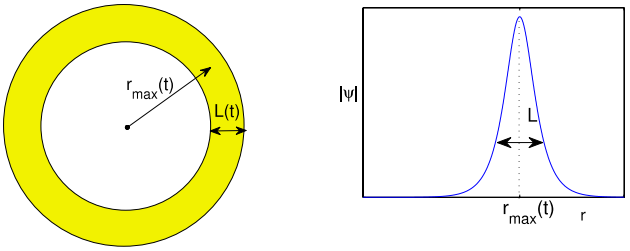

Fig. 2. Illustration of ring radius $r_{\max}(t)$ and width $L(t)$.

and

$$\alpha = \frac{2 - \sigma}{\sigma(d-1)}. \tag{7c}$$

The self-similar profile Q attains its global maximum at $\rho = 0$. Hence, $r_{\max}(t)$ is the ring radius and $L(t)$ is the ring width, see Fig. 2.

The ψ_Q ring solutions can be classified as follows, see Fig. 3:

A. In the subcritical case ($\sigma d < 2$), all NLS solutions globally exist, hence no singular ring solutions exist.
B. The critical case $\sigma d = 2$ corresponds to $\alpha = 1$. Since $r_{\max}(t) = r_0 L(t)$, these solutions undergo an *equal-rate collapse*, i.e., the ring radius goes to zero at the same rate as $L(t)$. The blowup rate of these critical ring solutions is a square root.
C. The supercritical case $2/d < \sigma < 2$ corresponds to $0 < \alpha < 1$. Therefore, the ring radius $r_{\max}(t) = r_0 L^\alpha(t)$ decays to zero, but at a slower rate than $L(t)$. The blowup rate of these ring solutions is
$$L(t) \sim \kappa(T_c - t)^p, \tag{8}$$
where $p = \frac{1}{1+\alpha} = \frac{\sigma(d-1)}{2+\sigma(d-2)}$.
D. The supercritical case $\sigma = 2$ corresponds to $\alpha = 0$. Since $r_{\max}(t) \equiv r_0$, the solution becomes singular on the d-dimensional sphere $|\mathbf{x}| = r_0$, rather than at a point. The blowup rate of these solutions is given by the loglog law (5).
E. The case $\sigma > 2$ was open until now.

Thus, the ψ_Q solutions are *shrinking rings* (i.e., $\lim_{t\to T_c} r_{\max}(t) = 0$) for $\frac{2}{d} \le \sigma < 2$ (cases B and C), and *standing rings* (i.e., $0 < \lim_{t\to T_c} r_{\max}(t) < \infty$) for $\sigma = 2$ (case D).

1.2. Singular standing-ring solutions of the NLS

One of the goals of this paper is to study singular ring-type solutions for $\sigma > 2$ (case E). The most natural guess is that these solutions also blowup with the ψ_Q profile. Since $\alpha < 0$ for $\sigma > 2$, see (7c), ψ_Q should be an *expanding ring*, i.e., $\lim_{t\to T_c} r_{\max} = \infty$. In this study we show that although such expanding rings do not violate power conservation, ψ_Q ring solutions cannot exist for $\sigma >$

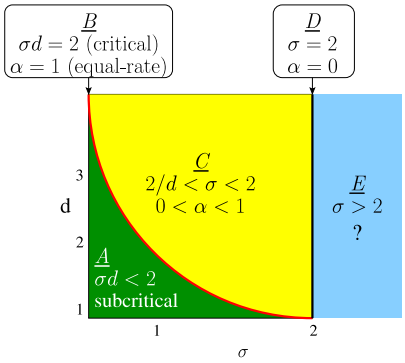

Fig. 3. Classification of singular ring solutions of the NLS as a function of σ and d. (A) subcritical case. (B) critical case, with equal-rate collapse [7]. (C) $2/d < \sigma < 2$, shrinking rings [2]. (D) $\sigma = 2$, standing rings [2,1,4]. (E) the case $\sigma > 2$, which is considered in this study.

2. Rather, singular rings solutions of the NLS (4) with $\sigma > 2$ are standing rings.

The blowup profile and rate of standing-ring solutions can be obtained using the following informal argument. In the ring region of a standing-ring, $\psi_{rr} \sim \frac{1}{L^2}$ and $\frac{1}{r}\psi_r \sim \frac{1}{L \cdot r_{\max}}$. Therefore, the $\frac{d-1}{r}\psi_r$ term in Eq. (4) becomes negligible compared with ψ_{rr} as $t \to T_c$. Hence, near the singularity, Eq. (4) reduces to the one-dimensional NLS[1]

$$\mathrm{i}\phi(t,x) + \phi_{xx} + |\phi|^{2\sigma}\phi = 0, \quad x = r - r_{\max}.$$

Therefore, the blowup profile and blowup-rate of standing-ring solutions of the NLS (4) with $d > 1$ and $\sigma \geq 2$ are the same as those of singular peak-type solutions of the one-dimensional NLS with the same σ. Specifically, standing-ring solutions are self-similar in the ring region, i.e., $\psi \sim \psi_F$, where ψ_F is, up to a shift in r, the asymptotic peak-type profile of the one-dimensional NLS, i.e.,

$$\psi_F(t, r - r_{\max}) = \phi_S(t,x),$$

and ϕ_S is given by (6a) with $d = 1$. In addition, the blowup rate $L(t)$ of ψ_F is the same as the blowup rate of ϕ_S, see (6c), and is equal to a square-root, i.e.,

$$L(t) \sim \kappa(\sigma)\sqrt{T_c - t}, \quad t \to T_c. \tag{9}$$

Moreover, $\kappa(\sigma)$ is universal, i.e., it depends on σ, but not on the dimension d or the initial condition ψ_0.

Numerically, we observe that ψ_F is an attractor for a large class of radially-symmetric initial conditions, but is unstable with respect to symmetry-breaking perturbations.

1.3. Singular standing vortex solutions of the NLS

The two-dimensional NLS

$$\mathrm{i}\psi_t(t,x,y) + \Delta\psi + |\psi|^{2\sigma}\psi = 0, \qquad \psi(0,x,y) = \psi_0(x,y),$$
$$\Delta = \partial_{xx} + \partial_{yy},$$

admits vortex solutions of the form $\psi(t,x,y) = A(t,r)\mathrm{e}^{\mathrm{i}m\theta}$, where $m \in \mathbb{Z}$. In [3], we presented a systematic study of singular vortex solutions. In particular, we showed that there exist singular vortex solutions that collapse with the asymptotic profile $\psi_Q \cdot \mathrm{e}^{\mathrm{i}m\theta}$, when ψ_Q is given by (7). The blowup rates of these solutions are the same as those of ψ_Q in the non-vortex case. Therefore, the $\psi_Q \cdot \mathrm{e}^{\mathrm{i}m\theta}$ vortex solutions can be classified as follows:

A. In the subcritical case ($\sigma < 1$), all NLS solutions globally exist, hence no singular vortex solutions exist.
B. In the critical case $\sigma = 1$, these solutions undergo an *equal-rate collapse* at a square root blowup rate.
C. The supercritical case $1 < \sigma < 2$ corresponds to $0 < \alpha < 1$. In this case, the ring radius decays to zero at a slower rate than $L(t)$ and the blowup rate is given by (8) where $p = \frac{1}{1+\alpha} = \frac{\sigma}{2}$.
D. The supercritical case $\sigma = 2$ corresponds to $\alpha = 0$. Therefore, the solution becomes singular on a circle. The blowup rate is given by the loglog law (5).
E. The case $\sigma > 2$ was open until now.

In this study, we show numerically that there exist singular standing-vortex solutions of the two-dimensional NLS with $\sigma > 2$ (case E) with the asymptotic profile $\mathrm{e}^{\mathrm{i}m\theta}\psi_F$. Moreover, the blowup rate of these singular standing vortices is the same as that of the standing-ring solutions in the non-vortex case, i.e., is given by (9). Therefore, these results extend the ones obtained in the non-vortex case.

1.4. Singular solutions of the biharmonic nonlinear Schrödinger equation

Let us consider the focusing biharmonic nonlinear Schrödinger equation (BNLS) equation

$$\mathrm{i}\psi_t(t,r) - \Delta^2\psi + |\psi|^{2\sigma}\psi = 0, \tag{10}$$

where Δ^2 is the radial biharmonic operator. Here, singularly formation is defined as $\lim_{t\to T_c}\|\psi\|_{H^2} = \infty$. In the *subcritical* case $\sigma d < 4$, all BNLS solutions exist globally [8]. Numerical simulations [8–10] indicate that in the *critical* case $\sigma = 4/d$ and the *supercritical* case $\sigma \geq 4/d$, the BNLS admits singular solutions. At present, however, there is no rigorous proof that the BNLS admits singular solutions, whether peak-type or ring-type.

Peak-type singular solutions of the BNLS (10) were recently studied numerically in [9,10]. The blowup rate of these solutions is slightly faster than $p = 1/4$ in the critical case ($1/4 + \log\log ?$), and is equal to $p = 1/4$ in the supercritical case.

The BNLS (10) also admits ring-type singular solutions for $4/d \leq \sigma \leq 4$ [11]. These solutions are of the form $\psi \sim \psi_{Q_B}$, where

$$|\psi_{Q_B}| = \frac{1}{L^{1/2\sigma}(t)}Q_B(\rho), \tag{11a}$$

$$\rho = \frac{r - r_{\max}(t)}{L(t)}, \quad r_{\max}(t) = r_0 L^{\alpha_B}(t), \tag{11b}$$

and

$$\alpha_B = \frac{4-\sigma}{\sigma(d-1)}. \tag{11c}$$

The ψ_{Q_B} solutions can be classified as follows (see Fig. 4):

A. In the subcritical case ($\sigma d < 4$), all BNLS solutions globally exist, hence no collapsing ring solutions exist.
B. The critical case $\sigma d = 4$ corresponds to $\alpha_B = 1$. These solutions undergo an *equal-rate collapse*. The blowup rate of these critical ring solutions is given by (8) with $p = 1/4$.
C. The supercritical case $4/d < \sigma < 4$ corresponds to $0 < \alpha_B < 1$. Therefore, the ring radius $r_{\max}(t) = r_0 L_B^{\alpha}(t)$ decays to zero, but at a slower rate than $L(t)$. The blowup rate of these ring solutions is given by (8) with $p = 1/(3+\alpha_B) = \sigma(d-1)/(4+3\sigma d - 4\sigma)$.

[1] Throughout this paper, we denote the solution of the one-dimensional NLS by ϕ, and its spatial variable by x.

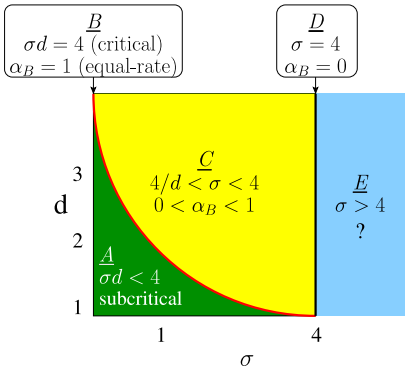

Fig. 4. Classification of singular ring solutions of the BNLS as a function of σ and d. (A) subcritical case. (B) critical case, with equal-rate collapse [11]. (C) $4/d < \sigma < 4$, shrinking rings [11]. (D) $\sigma = 4$, standing rings with the critical 1D profile [11]. (E) the case $\sigma > 4$, which is considered in this study.

D. The case $\sigma = 4$ corresponds to $\alpha_B = 0$. Since $r_{\max}(t) \equiv r_0$, the solution is a singular standing ring. The blowup rate is close to $p = 1/4$ and is conjectured to be $1/4$ with a loglog correction.
E. The case $\sigma > 4$ was open until now.

Thus, up to the change $\sigma \longrightarrow 2\sigma$, this classification is completely analogous to that of singular ring solutions of the NLS (see Fig. 3). In this work we show numerically that this analogy carries through to the regime $\sigma > 4$. Thus, the BNLS with $\sigma > 4$ and $d > 1$ admits singular standing-ring solutions. Near the standing-ring peak, Eq. (10) reduces to the one-dimensional BNLS

$$i\phi_t(t,x) - \phi_{xxxx} + |\phi|^{2\sigma}\phi = 0.$$

Therefore, the blowup profile and blowup-rate of standing ring solutions of the BNLS (10) with $d > 1$ and $\sigma \geq 4$ are the same as those of collapsing peak solutions of the one-dimensional BNLS with the same value of σ.

Thus, the results for ring solutions of the BNLS with $\sigma > 4$ are completely analogous, up to the change $\sigma \longrightarrow 2\sigma$, to those for singular standing-ring solutions of the NLS with $\sigma > 2$.

1.5. Singular solutions of the nonlinear heat equation

The d-dimensional nonlinear heat equation (NLHE)

$$u_t(t,r) - \Delta u - |u|^{2\sigma}u = 0, \quad \sigma > 0,\ d > 1, \tag{12}$$

admits singular solutions for any $\sigma > 0$ [12]. In [13], Giga and Kohn proved that (12) admits singular standing-ring solutions. Matos [14] proved that the blowup profile and blowup rate of these solutions are the same as those of singular peak-type solutions of the corresponding one-dimensional NLHE. We provide numerical evidence for the stability of these solutions.

1.6. Singular solutions of the biharmonic nonlinear heat equation

The d-dimensional nonlinear *biharmonic* heat equation (NLBHE)

$$u_t(t,r) + \Delta^2 u - |u|^{2\sigma}u = 0, \quad \sigma > 0,\ d > 1 \tag{13}$$

admits singular solutions for any $\sigma > 0$ [15]. To the best of our knowledge, until now all known singular solutions of (13) collapse at a point. In this study, we provide numerical evidence that the NLBHE (13) admits singular standing-ring solutions. The blowup profile and blowup rate of these solutions are the same as those of singular peak-type solutions of the corresponding one-dimensional equation.

1.7. Critical exponents of singular ring solutions

In Fig. 5A we plot the blowup rate parameter p of singular ring solutions of the NLS, see (8). As σ increases from $2/d$ to $2-$, p increases monotonically from $1/2$ to $1-$. When $\sigma = 2$, the blowup rate is given by the loglog law (5), i.e., $p = 1/2$ with a loglog correction. Finally, $p = 1/2$ for $\sigma > 2$. Since

$$\lim_{\sigma\to 2-} p = 1, \qquad \lim_{\sigma\to 2+} p = \frac{1}{2},$$

the blowup rate has a discontinuity at $\sigma = 2$. Surprisingly, the blowup rate is not monotonically-increasing with σ. For example, a ring solution of the NLS with $\sigma = 1.8$ blows up faster than a ring solution of the NLS with $\sigma = 2.2$.

The above results show that *the critical exponent of singular ring solutions of the NLS is* $\sigma = 2$: The blowup rate is discontinuous at $\sigma = 2$, and the blowup dynamics change from a shrinking-ring ($\sigma < 2$) to a standing-ring ($\sigma \geq 2$), see Fig. 5C. We can understand why $\sigma = 2$ is a critical exponent using the following argument. Standing-ring solutions are 'equivalent' to singular peak solutions of the one-dimensional NLS with the same nonlinearity exponent σ. Since $\sigma = 2$ is the critical exponent for singularity formation in the one-dimensional NLS, it is also a critical exponent for standing-ring blowup.

An analogous picture exists for the BNLS. For $4/d \leq \sigma < 4$, the blowup-rate p of the BNLS ring solutions increases monotonically in σ from $1/4$ to $(1/3)-$, at $\sigma = 4$, $p = 1/4$ possibly with a loglog correction, and $p = 1/4$ for $\sigma > 4$, see Fig. 5B. Therefore, the blowup rate is discontinuous at $\sigma = 4$. In addition, the blowup dynamics change at $\sigma = 4$ from a shrinking-ring ($\sigma < 4$) to a standing-ring ($\sigma > 4$), see Fig. 5D. Hence, *the critical exponent of standing-ring solutions of the BNLS is* $\sigma = 4$, precisely because it is the critical exponent for singularity formation in the one-dimensional BNLS.

In the case of the NLHE and BNLHE equations, there is no critical exponent of singular ring solutions. Indeed, these equations admit standing-ring solution for any $\sigma > 0$, precisely because there is no critical exponent for singularity formation in the corresponding one-dimensional equations.

1.8. Paper outline

The paper is organized as follows. In Section 2 we review the theory of singular peak-type solutions of the supercritical NLS, and conduct a numerical study of the one-dimensional case. In Section 3.1 we prove that standing-ring blowup can only occur for $\sigma \geq 2$, and show that the blowup profile and blowup-rate of singular standing ring solutions of the supercritical NLS with $\sigma > 2$ and $d > 1$ are the same as those of peak-type solutions of the one-dimensional NLS equation. In Section 3.2 we confirm these results numerically. We then show numerically that the singular standing-ring profile ψ_F is an attractor for radially-symmetric initial conditions (Section 3.3), but it is unstable with respect to symmetry-breaking perturbations (Section 3.4). In Section 4 we show analytically and numerically that expanding ψ_Q ring solutions do not exist for $\sigma > 2$. Section 5 extends the results to singular vortex solutions. In Section 6 we study singular peak-type solutions of the one-dimensional supercritical BNLS. In Section 7 we show that singular ring solutions of the supercritical BNLS with $\sigma > 4$ are standing-rings, whose blowup profile and blowup-rate are the same as those of peak-type solutions of the one-dimensional BNLS. In Section 8 we show that singular standing-ring solutions of the nonlinear heat equation exist for any $\sigma > 0$, and that their blowup profile and blowup-rate are the same as those of peak-type solutions of the one-dimensional NLHE. In

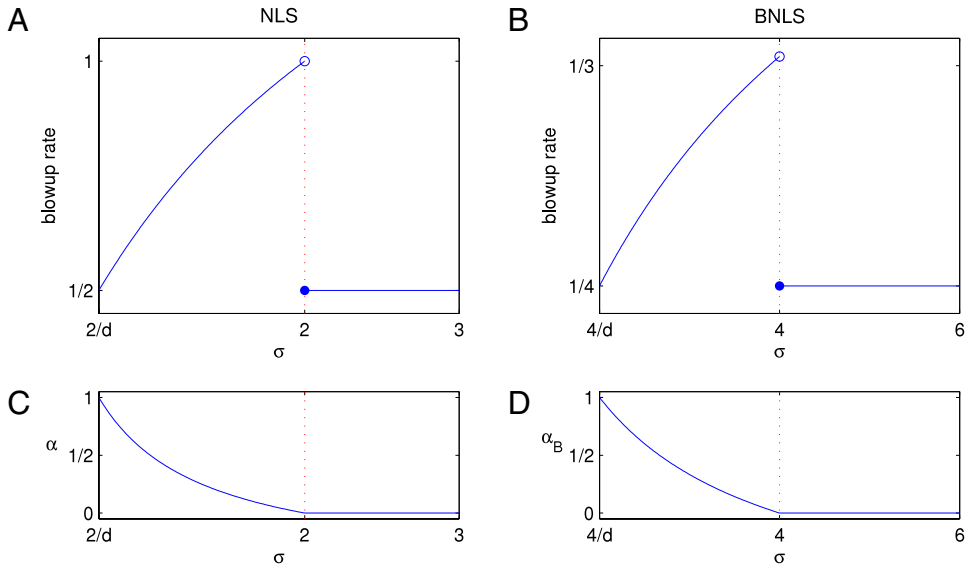

Fig. 5. (A) Blowup rate of singular ring solutions of the NLS. The blowup rate increases monotonically from $p = 1/2$ at $\sigma = 2/d$ to $p = 1-$ at $\sigma = 2-$. For $\sigma = 2$ (full circle) $p = 1/2$ (with a loglog correction) and for $\sigma > 2$, $p \equiv 1/2$. (B) Blowup rate of singular ring solutions of the BNLS. The blowup rate increases monotonically from $p = 1/4$ at $\sigma = 4/d$ to $p = (1/3)-$ at $\sigma = 4-$. For $\sigma = 4$ (full circle) $p = 1/4$ (with a loglog correction?) and for $\sigma > 4$, $p \equiv 1/4$. (C) The shrinkage parameter α, defined by the relation $r_{\max} \sim r_0 L^{\alpha}$ of singular ring solutions of the NLS. For $2/d \le \sigma < 2$, α decreases monotonically from 1 to 0+ (shrinking rings). For $\sigma \ge 2$, $\alpha \equiv 0$ (standing rings). (D) The shrinkage parameter α_B of singular ring solutions of the BNLS. For $4/d \le \sigma < 4$, α_B decreases monotonically from 1 to 0+ (shrinking rings). For $\sigma \ge 4$, $\alpha_B \equiv 0$ (standing rings).

Section 9 we show that singular standing-ring solutions of the nonlinear biharmonic heat equation exist for any $\sigma > 0$, and that their blowup profile and blowup-rate are the same as those of peak-type solutions of the one-dimensional BNLHE. The numerical methods used in this study are briefly described in Section 10.

Finally, we note that our results may be applicable to ring-type solutions of other equations, such as extinction solutions to the reaction–diffusion equation [16], and annular flames [17]. It is also instructive to compare the singular solutions of the NLS and the BNLS with those of the Keller–Segel equation, since although parabolic, it displays striking analogies with the NLS [18]. The Keller–Segel equation admits singular peak-type solutions in the two-dimensional critical case, and singular shrinking-ring solutions in the three-dimensional supercritical case [19,20]. No singular standing-ring solutions were found, however, for the multidimensional Keller–Segel equation. This is to be expected, as the one-dimensional Keller–Segel equation does not admit singular peak-type solutions.

2. Singular peak-type solutions of the one-dimensional supercritical NLS

2.1. Theory review

Let us consider the one-dimensional supercritical NLS

$$\mathrm{i}\phi_t(t,x) + \phi_{xx} + |\phi|^{2\sigma}\phi = 0, \quad \sigma > 2. \tag{14}$$

In contrast to the extensive theory on singularity formation in the critical NLS, much less is known about the supercritical case. Previous numerical simulations and formal calculations (see, e.g., [6, Chapter 7] and the references therein) suggested that peak-type singular solutions of the supercritical NLS (14) collapse with a self-similar asymptotic profile ϕ_S, i.e., $\phi \sim \phi_S$, where

$$\phi_S(t,x) = \frac{1}{L^{1/\sigma}(t)} S(\xi)\mathrm{e}^{\mathrm{i}\tau}, \quad \xi = \frac{x}{L(t)}, \ \tau = \int_0^t \frac{\mathrm{d}s}{L^2(s)}. \tag{15}$$

The blowup rate $L(t)$ of these solutions is a square root, i.e.,

$$L(t) \sim \kappa\sqrt{T_c - t}, \quad t \to T_c, \tag{16}$$

where $\kappa > 0$. In addition, the self-similar profile S is the solution of

$$S''(\xi) + \mathrm{i}\frac{\kappa^2}{2}\left(\frac{1}{\sigma}S + \xi S'\right) + |S|^{2\sigma}S = 0, \qquad S'(0) = 0, \qquad S(\infty) = 0. \tag{17}$$

In general, solutions of (17) are complex-valued, and depend on the parameter κ and on the initial condition $S(0)$. Solutions of (17) whose amplitude $|S|$ is monotonically-decreasing in ξ, and which have a zero Hamiltonian are called *admissible solutions* [6]. For each σ, Eq. (17) has a unique admissible solution (up to a multiplication by a constant phase $\mathrm{e}^{\mathrm{i}\alpha}$). This solution is attained for specific real values of κ and $S(0)$, which we denote as

$$\kappa = \kappa_S(\sigma), \qquad S(0) = S_0(\sigma). \tag{18}$$

Moreover, numerical simulations and formal calculations suggest that:

1. The self-similar profile of singular peak-type solutions of the NLS (14) is an admissible solution of (17).
2. The constant κ of the blowup rate (16) is universal (i.e., is independent of the initial condition ψ_0), and is equal to $\kappa_S(\sigma)$.

2.2. Simulations

To the best of our knowledge, the theory of supercritical peak-type collapse which is presented in Section 2.1, was tested numerically only for $d \ge 2$. Since this theory is not rigorous, and since we will make use of these results in Sections 3 and 4, we now confirm numerically the above theoretical predictions for the one-dimensional supercritical NLS (14).

We verified numerically that for each σ, there exists a unique admissible solution of (17). The corresponding values of κ_S and S_0 as a function of σ are shown in Fig. 6. For example, for $\sigma = 3$, the parameters of the admissible solution of Eq. (17) are

$$\kappa_S(\sigma = 3) \approx 1.664, \qquad S_0(\sigma = 3) \approx 1.155. \tag{19}$$

We now solve the one-dimensional NLS (14) with $\sigma = 3$ and the Gaussian initial condition $\phi_0(t = 0, x) = 2\mathrm{e}^{-2x^2}$. We first show

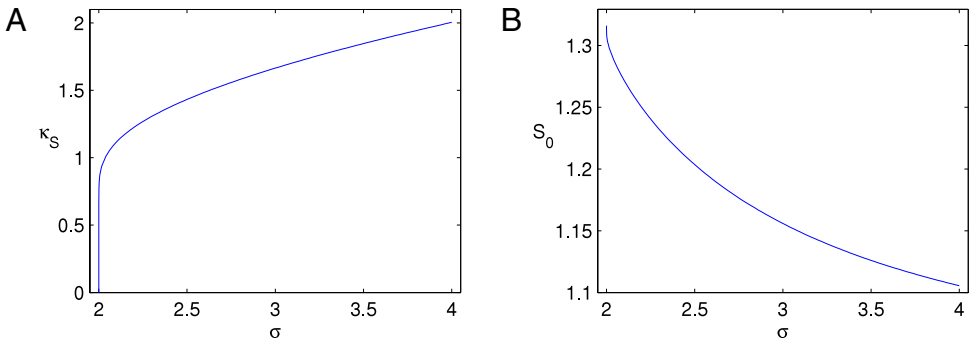

Fig. 6. The parameters κ_S and S_0 of the admissible solutions of Eq. (17), as function of σ.

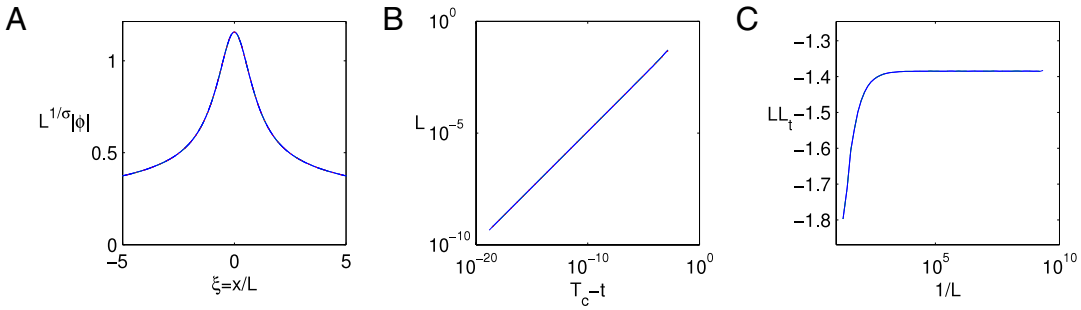

Fig. 7. Solution of the one-dimensional NLS (14) with $\sigma = 3$ and the initial condition $\psi_0 = 2e^{-2x^2}$. (A) Rescaled solution, see (20), at the focusing levels $1/L = 10^4$ (solid) and $1/L = 10^8$ (dashed); the dotted curve is the admissible profile $S(\xi;\sigma=3)$, all three curves are indistinguishable. (B) L as a function of $(T_c - t)$ on a logarithmic scale. The dotted curve is the fitted curve $1.713 \cdot (T_c - t)^{0.5007}$. The two curves are indistinguishable. (C) LL_t as a function of $1/L$.

that the NLS solution collapses with the self-similar profile ϕ_S, see (15). To do that, we rescale the solution according to

$$\phi_{\text{rescaled}}(t,x) = L^{\frac{1}{\sigma}(t)} \left|\phi\left(\frac{x}{L(t)}\right)\right| \qquad L(t) = \left(\frac{\|S\|_\infty}{\|\phi\|_\infty}\right)^\sigma = \left(\frac{S_0^{1D}(\sigma)}{\|\phi\|_\infty}\right)^\sigma. \tag{20}$$

The rescaled profiles at focusing levels of $1/L = 10^4$ and $1/L = 10^8$ are indistinguishable, see Fig. 7A, indicating that the solution is indeed self-similar while focusing over 4 orders of magnitude. Moreover, the rescaled profiles are in perfect fit with the admissible $S(\xi;\sigma=3)$ profile.

Next, we consider the blowup rate of ϕ. To do that, we first assume that

$$L(t) \sim \kappa (T_c - t)^p, \tag{21}$$

and find the best fitting κ and p, see Fig. 7B. In this case $\kappa \approx 1.713$ and $p \approx 0.5007$, indicating that the blowup rate is square-root or slightly faster. In order to check whether L is slightly faster than a square root, we compute the limit $\lim_{t\to T_c} LL_t$, see [7]. Recall that for the square-root blowup rate (16),

$$\lim_{t\to T_c} LL_t = -\frac{\kappa^2}{2} < 0,$$

while for a faster-than-a-square root blowup rate LL_t goes to zero. Since $\lim_{T_c\to t} LL_t = -1.384$, see Fig. 7C, the blowup rate of ϕ is square-root (with no loglog correction), i.e.,

$$L(t) \sim \kappa_{1D}^{\text{blowup-rate}} \sqrt{T_c - t}, \qquad \kappa_{1D}^{\text{blowup-rate}} \approx \sqrt{2 \cdot 1.384} \approx 1.664. \tag{22}$$

In particular, there is an excellent match (to 4 digits) between $\kappa_{1D}^{\text{blowup-rate}} \approx 1.664$ extracted from the blowup rate of ϕ, see (22) and the parameter $\kappa_S(\sigma=3)$ of the admissible $S(\xi;\sigma=3)$ profile, see (19).

3. Singular standing-ring solutions of the supercritical NLS

Let us consider singular solutions of the supercritical NLS

$$i\psi_t(t,r) + \psi_{rr} + \frac{d-1}{r}\psi_r + |\psi|^{2\sigma}\psi = 0, \quad d > 1,\ \sigma d > 2. \tag{23}$$

In this section we show that Eq. (23) has singular standing-ring solutions for $\sigma \geq 2$. Since the case $\sigma = 2$ was already studied in [2,1,4], we mainly focus on the case $\sigma > 2$.

3.1. Analysis

The following lemma shows that standing-ring blowup can only occur for $\sigma \geq 2$:

Lemma 1. *Let ψ be a standing-ring singular solution of the NLS (23), i.e., $\psi \sim \psi_F$ for $|r - r_{\max}| \leq \rho_c \cdot L(t)$, where*

$$|\psi_F(t,r)| = \frac{1}{L^{1/\sigma}(t)}|F(\rho)|, \qquad \rho = \frac{r - r_{\max}(t)}{L(t)}, \tag{24a}$$

$$\lim_{t\to T_c} L(t) = 0,$$

and

$$0 < \lim_{t\to T_c} r_{\max}(t) < \infty. \tag{24b}$$

Then, $\sigma \geq 2$.

Proof. The power of the collapsing part ψ_F is

$$\begin{aligned}\|\psi_F\|_2^2 &= L^{-2/\sigma}\int_{r=r_{\max}-\rho_c\cdot L(t)}^{r_{\max}+\rho_c\cdot L(t)} \left|F\left(\frac{r-r_{\max}}{L}\right)\right|^2 r^{d-1}\mathrm{d}r \\ &= L^{-2/\sigma}\int_{\rho=-\rho_c}^{\rho_c} |F(\rho)|^2 (L\rho + r_{\max})^{d-1}(L\mathrm{d}\rho) \\ &\sim L^{1-2/\sigma}(t)\cdot r_{\max}^{d-1}\int_{\rho=-\rho_c}^{\rho_c}|F(\rho)|^2\,\mathrm{d}\rho.\end{aligned}$$

Since $\|\psi_F\|_2^2 \le \|\psi\|_2^2 = \|\psi_0\|_2^2 < \infty$, then $L^{1-2/\sigma}$ has to be bounded as $L \to 0$, hence $\sigma \ge 2$. □

Let

$$P_{\text{collapse}} = \liminf_{\varepsilon\to 0+} \lim_{t\to T_c} \int_{|r-r_{\max}(t)|<\varepsilon} |\psi|^2 r^{d-1} dr$$

be the amount of power that collapses into the standing-ring singularity. We say that a singular standing-ring solution ψ undergoes a *strong collapse* if $P_{\text{collapse}} > 0$, and a *weak collapse* if $P_{\text{collapse}} = 0$.

Corollary 2. *Under the conditions of Lemma 1, ψ_F undergoes a strong collapse when $\sigma = 2$, and a weak collapse when $\sigma > 2$.*

Proof. This follows directly from the proof of Lemma 1. □

Let us further consider singular standing-ring solutions of the NLS (23). Following the analysis in [2, Section 3.2], in the ring region of a standing-ring solution, i.e., for $r - r_{\max} = \mathcal{O}(L)$,

$$[\psi_{rr}] \sim \frac{[\psi]}{L^2(t)}, \qquad \left[\frac{d-1}{r}\psi_r\right] \sim \frac{(d-1)[\psi]}{r_{\max}(T_c)\cdot L(t)}.$$

Therefore, the $\frac{d-1}{r}\psi_r$ term in Eq. (23) becomes negligible compared with ψ_{rr} as $t \to T_c$.

Hence, near the singularity, Eq. (23) reduces to the one-dimensional supercritical NLS (14), i.e.,

$$\psi(t, r) \sim \phi\left(t, x = r - r_{\max}(t)\right),$$

where ϕ is a peak-type solution of the one-dimensional NLS (14).

Therefore, we predicted in [2] that the blowup dynamics of standing ring solutions of the NLS (23) with $d > 1$ and $\sigma = 2$ is the same as the blowup dynamics of collapsing peak solutions of the one-dimensional critical NLS with $\sigma = 2$, as was indeed confirmed numerically in [2] and analytically in [1,4]. Similarly, we now predict that the blowup dynamics of standing-ring solutions of the NLS (23) with $d > 1$ and $\sigma > 2$ is the same as the blowup dynamics of collapsing peak solutions of the supercritical one-dimensional NLS (14) with the same nonlinearity exponent σ:

Conjecture 3. *Let ψ be a singular standing-ring solution of the NLS equation (23) with $d > 1$ and $\sigma > 2$. Then,*

1. *The solution is self-similar in the ring region, i.e., $|\psi| \sim |\psi_F|$ for $r - r_{\max} = \mathcal{O}(L)$, where ψ_F is given by (24a).*
2. *The self-similar profile ψ_F is given by*

$$\psi_F(t, r) = \phi_S\left(t, x = r - r_{\max}(t)\right), \tag{25}$$

where $\phi_S(t, x)$, see (15), is the asymptotic peak-type profile of the one-dimensional NLS (14) with the same σ. In particular, $F = S$ is the admissible solution of Eq. (17) with

$$\kappa = \kappa_S(\sigma), \qquad S_0 = S_0(\sigma).$$

3. *The blowup rate of ψ is a square root, i.e.,*

$$L(t) \sim \kappa_S(\sigma)\sqrt{T_c - t}, \quad t \longrightarrow T_c, \tag{26}$$

where $\kappa_S(\sigma)$, is the parameter $\kappa = \kappa_S$ of the self-similar profile S, see (18).

Conjecture 3 implies that the parameter κ of the blowup-rate (26) of ψ is equal to the parameter κ of the blowup rate (16) of ϕ. In particular, κ depends on the nonlinearity exponent σ, but is independent of the dimension d and of the initial condition ψ_0.

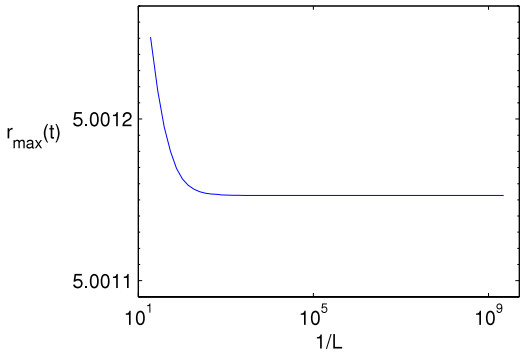

Fig. 8. Ring radius $r_{\max}(t)$ as a function of the focusing level $1/L(t)$ for the solution of the NLS (23) with $d = 2$ and $\sigma = 3$, and the initial condition (27).

3.2. Simulations

We solve the NLS (23) with $d = 2$ and $\sigma = 3$ for the initial condition

$$\psi_0 = 2e^{-2(r-5)^2}, \tag{27}$$

and observe that the solution blows-up with a ring profile. In Fig. 8 we plot the ring radius

$$r_{\max}(t) = \arg\max_r |\psi|$$

as a function of the focusing factor $1/L(t)$, as the solution blows up over 10 orders of magnitude. Since $\lim_{t\to T_c} r_{\max}(t) = 5.0011$, the ring is standing and is not shrinking or expanding.

We now test Conjecture 3 numerically item by item.

1. In Fig. 7A we plot the rescaled solution

$$\psi_{\text{rescaled}} = L^{\frac{1}{\sigma}}(t)\left|\psi\left(\frac{r - r_{\max}(t)}{L(t)}\right)\right|,$$
$$L(t) = \left(\frac{S_0(\sigma)}{\|\psi(t)\|_\infty}\right)^\sigma, \tag{28}$$

   at $1/L = 10^4$ and $1/L = 10^8$, and observe that the two lines are indistinguishable. Therefore, we conclude that the standing-ring solutions blowup with the self-similar ψ_F profile (24a).
2. To verify that the self-similar blowup profile ψ_F is, up to a shift in r, the asymptotic blowup peak-profile ϕ_S of the one-dimensional NLS (14), we superimpose in Fig. 9A the self-similar profile of the solution of the one-dimensional NLS (14) from Fig. 7A and the admissible solution $S(x, \sigma = 3)$, and observe that, indeed, the four curves are indistinguishable.
3. Fig. 9B shows that

$$L(t) \sim 1.714 \cdot (T_c - t)^{0.5009}.$$

   Therefore, the blowup rate is a square-root or slightly faster. Fig. 9C shows that $\lim_{T_c\to t} LL_t \approx -1.385$, indicating that the blowup rate is square-root (with no loglog correction), i.e.,

$$L(t) \sim \kappa_{2D}^{\text{blowup-rate}}\sqrt{T_c - t},$$
$$\kappa_{2D}^{\text{blowup-rate}} = \sqrt{2 \cdot 1.385} \approx 1.664. \tag{29}$$

   Thus, there is an excellent match between the parameter $\kappa = \kappa_S(\sigma = 3) \approx 1.664$ of the admissible S profile, see (19), the value of $\kappa_{2D}^{\text{blowup-rate}} \approx 1.664$ extracted from the blowup rate of the solution of the two-dimensional NLS, and the value of $\kappa_{1D}^{\text{blowup-rate}} \approx 1.664$ extracted from the blowup rate of the solution of the one-dimensional NLS, see (22).

3.3. Robustness of ψ_F and universality of κ

The initial condition (27) in Figs. 8 and 9 is different from the asymptotic profile ψ_F. Since the solution ψ blows up with the

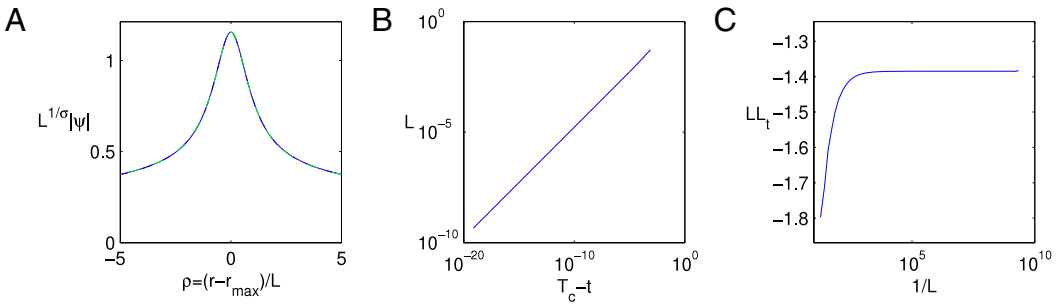

Fig. 9. NLS solution of Fig. 8. (A) Rescaled solution according to (28) at focusing levels $1/L = 10^4$ (solid) and $1/L = 10^8$ (dashed), the dotted curve is the asymptotic profile $S(\xi, \sigma = 3)$, and the dashed curve is the rescaled solution of the one-dimensional NLS at $1/L = 10^8$, taken from Fig. 7A. All four curves are indistinguishable. (B) L as a function of $(T_c - t)$ on a logarithmic scale. The dotted curve is the fitted curve $1.709(T_c - t)^{0.5007}$. (C) LL_t as a function of $1/L$.

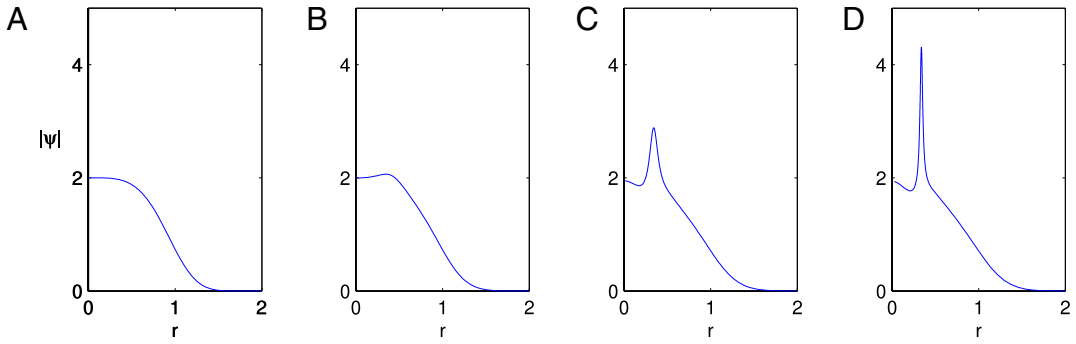

Fig. 10. Solution of the NLS (23) with $d = 2$ and $\sigma = 3$ and the initial condition $\psi_0 = 2e^{-r^4}$ at (A) $t = 0$. (B) $t = 0.0105$. (C) $t = 0.0188$. (D) $t = 0.0198$.

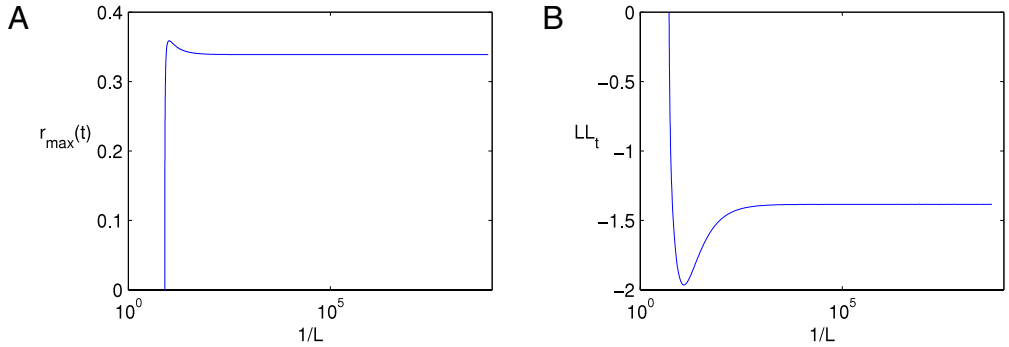

Fig. 11. NLS solution of Fig. 10. (A) Location of the maximum $r_{\max}(t)$ as a function of the focusing level $1/L(t)$ (B) LL_t as a function of the focusing level $1/L(t)$.

asymptotic profile ψ_F, this indicates that ψ_F is an attractor. The initial condition (27), however, is already ring-shaped. Therefore, we now show that initial conditions which are not ring-shaped can also blowup with the ψ_F profile.

In [21,22], we developed a Nonlinear Geometrical Optics (NGO) method which showed that high-power super-Gaussian initial conditions evolve into a ring profile. To see this, in Fig. 10 we solve the NLS (3) with $d = 2$ and $\sigma = 3$, and the super-Gaussian initial condition $\psi_0(r) = 2e^{-r^4}$, and observe that the NLS solution, indeed, evolves into a ring. Since $\lim_{t\to T_c} r_{\max}(t) = 0.33$, see Fig. 11A, this singular solution is a standing ring. Therefore, we see that initial conditions which are not rings can also blowup with the ψ_F standing ring profile.

We now consider the blowup rate of the above solution, since $\lim_{t\to T_c} LL_t = -1.384$, see Fig. 11B, this implies that

$$L(t) \sim \kappa_{2D}^{\text{blowup-rate}} \sqrt{T_c - t}, \quad \kappa_{2D}^{\text{blowup-rate}} \approx \sqrt{2 \cdot 1.384} = 1.664.$$

This value of $\kappa_{2D}^{\text{blowup-rate}}$ identifies with the one obtained for the ring-type initial condition (27), see (29). We thus see that the parameter κ of the blowup rate (26) is, indeed, independent of the initial condition.

Remark 3.1. A different type of initial condition that blows-up with the ψ_F profile and with the same value of $\kappa_{2D}^{\text{blowup-rate}}$ is given in Section 4.2.

3.4. Instability with respect to symmetry-breaking perturbations

In Section 3.3 we saw that the standing-ring asymptotic profile ψ_F is an attractor for a large class of radially-symmetric initial conditions. In general, NLS solutions with a ring structure are stable under radial perturbation, but unstable under symmetry-breaking perturbations [7,2,3]. We now show that ψ_F is also unstable with respect to symmetry-breaking perturbations. To see that, let us consider the two-dimensional NLS

$$i\psi_t(t, r, \theta) + \psi_{rr} + \frac{1}{r}\psi_r + \frac{1}{r^2}\psi_{\theta\theta} + |\psi|^{2\sigma}\psi = 0, \tag{30}$$

with the initial condition

$$\psi_0(r, \theta) = f(r)\,(1 + \varepsilon h(\theta))\,.$$

We chose $f(r)$ so that when $\varepsilon = 0$, the solution blows up with the ψ_F profile at $r = r_{\max}$. We now consider the case $0 < \varepsilon \ll 1$. Since for a standing ring the $\frac{1}{r}\psi_r$ term becomes negligible compared

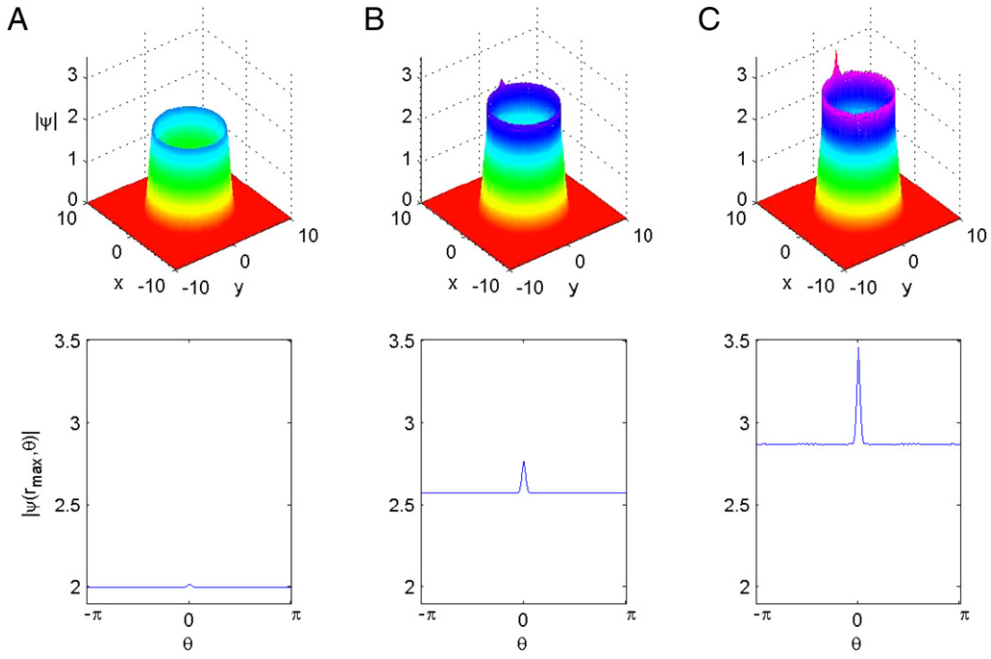

Fig. 12. Solution of the NLS (30) with $\sigma = 3$ and with the initial condition (31). (A) $t = 0$. (B) $t = 0.01400$, (C) $t = 0.01472$. Top: Surface plot. Bottom: Amplitude along the ring peak $|\psi(t, r_{\max}(t), \theta)|$ as function of θ.

with ψ_{rr}, see Section 3.1, Eq. (30) can be approximated in the ring-peak region ($r \approx r_{\max}$) with

$$i\psi_t + \psi_{rr} + \frac{1}{r_{\max}^2}\psi_{\theta\theta} + |\psi|^{2\sigma}\psi = 0.$$

This is the two-dimensional focusing NLS. Therefore, the solution will localize at local maximum points in the (r, θ) plane, thereby breaking the radial symmetry.

To see this numerically, we solve the two-dimensional NLS (30) with $\sigma = 3$ and with the initial condition

$$\psi_0(r, \theta) = 2e^{-2(r-5)^2}\left[1 + \varepsilon^2 e^{-\left(\frac{\theta}{\varepsilon}\right)^2}\right],$$

$$\varepsilon = \frac{1}{10},\ \theta = [-\pi, \pi]. \tag{31}$$

This initial condition is the standing-ring initial condition (27), with an $\mathcal{O}(0.01)$ small bump at $\theta = 0$, see Fig. 12A. As predicted, as the solution self-focuses, it localizes around the small initial bump at $\theta = 0$ (see Fig. 12B and C), resulting in breakup of radial symmetry.

4. Existence of non-standing ring solutions for $\sigma > 2$?

Lemma 1 does not exclude the possibility that there exist non-standing rings for $\sigma > 2$. The main reason that this question arises is as follows. In [2] we discovered ring solutions of the supercritical NLS for $d > 1$ and $\frac{2}{d} < \sigma \leq 2$ of the form $\psi \sim \psi_Q$, see (7). Therefore, it is natural to attempt to extrapolate these results to the regime $\sigma > 2$. Since $\alpha < 0$ when $\sigma > 2$, the ring radius $r_{\max}(t)$ goes to infinity as $t \to T_c$, hence ψ_Q is an *expanding-ring* profile for $\sigma > 2$, if such a solution exists. Note that although the ring is expanding to an infinite radius, the power of the collapsing part ψ_Q remains bounded, as

$$\|\psi_Q\|_2^2 = \int_{r=r_{\max}-\rho_c\cdot L(t)}^{r_{\max}+\rho_c\cdot L(t)} |\psi_Q|^2 r^{d-1} dr \sim r_0^{d-1}\int_{\rho=-\rho_c}^{\rho_c} |Q|^2 d\rho,$$
$$t \to T_c.$$

Therefore, these expanding rings, if they exist, do not violate power conservation.

In [2] we solved the NLS (23) with $\sigma = 2.1 > 2$ and $d = 2$ and the ring initial condition $\psi_0 = \sqrt[4]{3}\sqrt{\mathrm{sech}(2(r-5))}$. The solution turned out to be a singular standing ring, rather than an expanding one. Moreover, the blowup profile was different from ψ_Q. In retrospect, this NLS solution was a standing-ring with the ψ_F profile, see Section 3. Nevertheless, this still leaves open the question of whether there exist expanding-ring ψ_Q solutions for $\sigma > 2$.

4.1. Analysis

We now prove that singular ring solutions with the ψ_Q profile do not exist for $\sigma > 2$.

Lemma 4. *When $\sigma > 2$, there are no singular NLS solutions such that $\psi \sim \psi_Q$, see (7), and*

$$L(t) \sim \kappa(T_c - t)^p, \qquad L_t \sim p\kappa(T_c - t)^{p-1},$$
$$L_{tt} \sim p(p-1)\kappa(T_c - t)^{p-2}. \tag{32}$$

Proof. The result shall follow directly from Lemmas 5 and 6. □

Lemma 5. *Under the assumptions of Lemma 4, $p < 1$.*

Proof. We first recall that, as shown by Merle [23], for every singular solution ψ of the supercritical NLS

$$\int_0^{T_c} (T_c - t)\|\nabla\psi\|_2^2 dt < \infty. \tag{33}$$

To find the limiting behavior of $\|\nabla\psi(t)\|_2^2$ as $t \to T_c$, note that by the conservation of the Hamiltonian

$$\|\nabla\psi\|_2^2 \sim \frac{1}{\sigma+1}\|\psi\|_{2\sigma+2}^{2\sigma+2}, \quad t \to T_c. \tag{34}$$

In addition,

$$\|\psi\|_{2\sigma+2}^{2\sigma+2} \sim \|\psi_Q\|_{2\sigma+2}^{2\sigma+2} = \frac{1}{L^{\frac{2\sigma+2}{\sigma}}}\int |Q(\rho)|^{2\sigma+2}(L\rho + r_0 L^\alpha)^{d-1} L d\rho$$
$$\sim \frac{r_0^{d-1}}{1+\sigma}\frac{1}{L^2(t)}\int |Q|^{2\sigma+2} d\rho, \tag{35}$$

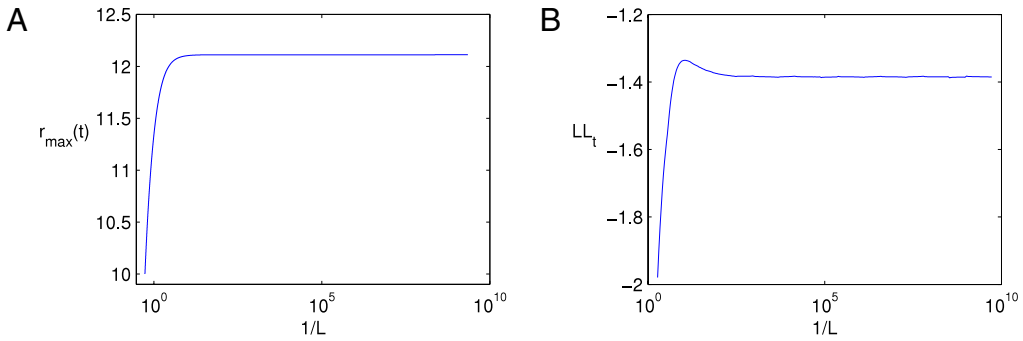

Fig. 13. Solution of the NLS (23) with $d = 2$ and $\sigma = 3$ and the initial condition (38). (A) Ring radius $r_{\max}(t)$ as a function of the focusing level $1/L(t)$. (B) LL_t as a function of $1/L$.

where in the last equality we used the value of α given by (7c), and, in particular, that $\alpha < 0$. Therefore, by (32), (34), (35)

$$\|\nabla\psi\|_2^2 \sim \|\psi\|_{2\sigma+2}^{\sigma+1} \sim \frac{1}{L^2(t)} \sim \frac{1}{(T_c - t)^{2p}}, \quad t \to T_c.$$

Hence, the bound (33) implies that $p < 1$. □

Lemma 6. *Under the conditions of Lemma 4, $p > 1$.*

Proof. Substitution of ψ_Q, see (7), into the NLS (23) gives the following ODE for Q,

$$Q_{\rho\rho}(\rho) + \frac{(d-1)L}{L\rho + r_0 L^\alpha} Q_\rho - Q + |Q|^{2\sigma} Q - \left[A(t)\rho^2 + \alpha r_0 B(t)\rho + \alpha r_0^2 C(t)\right] Q + \mathrm{i}D(t)Q = 0, \tag{36a}$$

where

$$A(t) = \frac{1}{4}L^3 L_{tt}, \qquad B(t) = \frac{1}{2}L^{2+\alpha}L_{tt} - 2(1-\alpha)L^{1+\alpha}L_t^2,$$
$$C(t) = \frac{1}{4}L^{1+2\alpha}L_{tt} - (1-\alpha)L^{2\alpha}L_t^2,$$
$$D(t) = \frac{\sigma d - 2}{2\sigma}\frac{LL_t}{\rho + r_0 L^{\alpha-1}}\rho.$$

Since Q depends only on ρ, each of the time-dependent terms of (36) should go to a constant as $t \to T_c$. In particular, $C(t)$ should go to a constant as $t \to T_c$. Under assumption (32),

$$C(t) \sim c_C (T_c - t)^{2\alpha p + 2p - 2}, \quad c = \kappa^{2+2\alpha} p \left[\left(\alpha - \frac{3}{4}\right)p - \frac{1}{4}\right]. \tag{37}$$

Since $\lim_{t\to T_c} L(t) = 0$, then $p > 0$, see (32). In addition, for $\sigma > 2$, $\alpha < 0$, see (7c). This implies that $c < 0$ and in particular $c \neq 0$. Since $C(t)$ should goes to a constant as $t \to T_c$ then, by (37), $2\alpha p + 2p - 2 \geq 0$. Therefore,

$$\frac{1-p}{p} \leq \alpha < 0.$$

Hence, $p > 1$. □

4.2. Simulations

The result of Lemma 4 that expanding-ring singular solutions with the profile ψ_Q do not exist, is based on formal arguments rather than on a rigorous analysis. Therefore, we now provide a numerical support for this result. To do that, we solve the NLS (23) with $d = 2$ and $\sigma = 3$ and with the expanding ring profile initial condition

$$\psi_0 = \psi_Q(t=0) = (1+\sigma)^{\frac{1}{2\sigma}} \operatorname{sech}^{\frac{1}{\sigma}}(\sigma(r-10)) \times \mathrm{e}^{-\mathrm{i}\alpha r^2 - \mathrm{i}(1-\alpha)(r-10)^2}, \tag{38a}$$

where

$$\alpha = \frac{2-3}{3(2-1)} = -\frac{1}{3}. \tag{38b}$$

If a ψ_Q solution indeed exists, then ψ would be a singular ring solution whose radius goes to infinity. In Fig. 13A we plot the ring radius $r_{\max}(t)$ as a function of the focusing factor $1/L$, as the solution blows up over 10 orders of magnitude. Initially, the ring radius, indeed, expands from $r_{\max}(0) = 10$ to $r_{\max}(t) \approx 12.11$. This expansion is due to the defocusing (expanding) phase term $\mathrm{e}^{-\mathrm{i}\alpha r^2}$ of the initial condition. However, the ring stops expanding when $1/L \approx 20$, and becomes a singular standing ring with radius $r_{\max}(T_c) \approx 12.11$. Since the initial condition was an expanding ring, this simulation provides a strong support to the result of Lemma 4.

We now consider the blowup rate of the above solution, Fig. 13B shows that $\lim_{t\to T_c} LL_t = -1.384$, implying that

$$L(t) \sim \kappa_{2D}^{\text{blowup-rate}} \sqrt{T_c - t}, \quad \kappa_{2D}^{\text{blowup-rate}} \approx \sqrt{2 \cdot 1.384} = 1.664.$$

This value of $\kappa_{2D}^{\text{blowup-rate}}$ identifies with the one obtained for a ψ_F collapse, see (29). Therefore, this simulation provides an additional support to the robustness of ψ_F and to the universality of κ (see Section 3.3).

5. Singular standing vortex solutions of the NLS ($\sigma > 2$)

We now consider vortex solutions of the two-dimensional NLS

$$\mathrm{i}\psi_t(t,x,y) + \Delta\psi + |\psi|^{2\sigma}\psi = 0, \qquad \psi(0,x,y) = \psi_0(x,y), \quad \Delta = \partial_{xx} + \partial_{yy}, \tag{39}$$

i.e., solutions of the form

$$\psi(t,r,\theta) = A(t,r)\mathrm{e}^{\mathrm{i}m\theta}, \quad m \in \mathbb{Z}, \tag{40}$$

where $r = \sqrt{x^2+y^2}$ and $\theta = \tan^{-1}(x/y)$.

In [3] we proved that if the initial condition is a radially-symmetric vortex, then the solution remains a vortex:

Lemma 7. *Let ψ be a solution of the NLS (39) with the initial condition $\psi_0(r,\theta) = A_0(r)\mathrm{e}^{\mathrm{i}m\theta}$. Then, $\psi(t,r,\theta) = A(t,r)\mathrm{e}^{\mathrm{i}m\theta}$, where $A(t,r)$ is the solution of*

$$\mathrm{i}A_t(t,r) + A_{rr} + \frac{1}{r}A_r - \frac{m^2}{r^2}A + |A|^{2\sigma}A = 0, \qquad A(0,r) = A_0(r). \tag{41}$$

Note that the phase singularity at $r = 0$ implies that $A(r = 0) = 0$. Hence, all vortex solutions are ring-type solutions. Specifically, all the singular solutions of (41) are ring-type and not peak-type.

In [3] we showed by formal calculations and numerical simulations that Eq. (39) admits singular shrinking-vortex solutions for

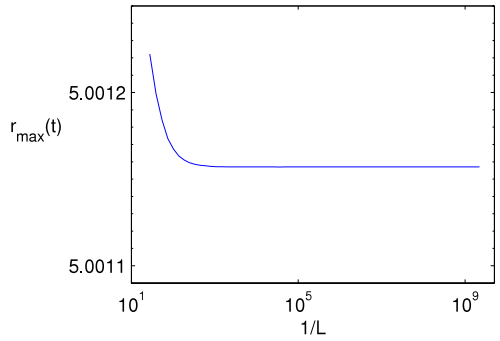

Fig. 14. Ring radius $r_{\max}(t)$ as a function of the focusing level $1/L(t)$ for the solution of the two-dimensional NLS (23) with $m = 1$, $\sigma = 3$ and the initial condition (43).

$1 \le \sigma < 2$, and singular standing-vortex solutions for $\sigma = 2$. Moreover, we showed that the blowup rate and profile of the standing-vortex solutions is the same as in the two-dimensional non-vortex case. We now show that this is also true for $\sigma > 2$, namely, that the analysis conducted in Section 3.1 for non-vortex standing-ring collapse, applies also for singular standing-vortex solutions.

5.1. Analysis

Lemma 8. *Let ψ be a singular standing-ring vortex solution of the NLS (39), i.e., $\psi \sim \psi_F(t,r)e^{im\theta}$, where ψ_F is given by (24a). Then, $\sigma \ge 2$.*

Proof. The proof is identical to the proof of Lemma 1. Indeed, the proof of Lemma 1 relies only on $|\psi|$, hence is not affected by the phase term $e^{im\theta}$. □

We now show that the blowup dynamics of standing vortex solutions is the same as the blowup dynamics of collapsing solutions of the one-dimensional NLS (14). Indeed, in the ring region of a standing vortex solution,

$$[A_{rr}] \sim \frac{[A]}{L^2(t)}, \qquad \left[\frac{d-1}{r}A_r\right] \sim \frac{(d-1)[A]}{r_{\max}(T_c)\cdot L(t)},$$
$$\left[\frac{m^2}{r^2}A\right] \sim \frac{m^2[A]}{r^2_{\max}(T_c)}.$$

Therefore, as $t \to T_c$, both the $\frac{d-1}{r}A_r$ and $\frac{m^2}{r^2}A$ terms in Eq. (23) become negligible compared with A_{rr}.

Hence, as in the non-vortex case, near the singularity, Eq. (23) reduces to the one-dimensional NLS (14), i.e.,

$$A(t,r) \sim \phi\,(t, x = r - r_{\max}(t))\,, \tag{42}$$

where ϕ is a peak-type solution of the one-dimensional NLS (14). Therefore, we expect that the blowup dynamics of standing-vortex solutions of the NLS (23) with $d = 2$ and $\sigma > 2$ to be the same as the blowup dynamics of collapsing peak solution of the one-dimensional NLS (14) with the same nonlinearity exponent σ:

Conjecture 9. *Let $\psi(t,r,\theta) = A(t,r)e^{im\theta}$ be a singular standing-vortex solution of the NLS equation (39) with $\sigma > 2$. Then, ψ blows up with the asymptotic self-similar profile*

$$\psi \sim e^{im\theta}\cdot\psi_F(t,r),$$

where ψ_F is given by (25). In addition, items 1–3 *of Conjecture* 3 *hold.*

5.2. Simulations

We solve Eq. (41) with $m = 1$ and $\sigma = 3$, with the initial condition

$$A_0 = 2\tanh(4r^2)e^{-2(r-5)^2}. \tag{43}$$

In Fig. 14 we plot the ring radius $r_{\max}(t)$ as a function of the focusing factor $1/L(t)$, as the solution blows up over 10 orders of magnitude. Since $\lim_{t\to T_c} r_{\max}(t) = 5.0011$, the vortex is standing.

We now test Conjecture 9 numerically item by item.

1. In Fig. 15 we plot the rescaled solution, see Eq. (28), at $1/L = 10^4$ and $1/L = 10^8$, and observe that, indeed, the standing ring solution undergoes a self-similar collapse with the profile (25).
2. To verify that the self-similar collapse profile is, up to a shift in r and multiplication by $e^{im\theta}$, the asymptotic collapse profile ϕ_S of the one-dimensional NLS (14), we superimpose the rescaled solution of the one-dimensional NLS (14) from Fig. 7A, as well as the admissible solution $S(x, \sigma = 3)$, on to the rescaled solutions of Fig. 15A and observe that, indeed, the four curves are indistinguishable.
3. Fig. 15B shows that

   $$L(t) \sim 1.701\cdot(T_c - t)^{0.50068}.$$

   Therefore, the blowup rate is square root or slightly faster. Fig. 15C shows that

   $$\lim_{T_c\to t} LL_t \approx -1.384,$$

   indicating that the blowup rate is square-root, i.e.,

   $$L(t) \sim \kappa_{2D\text{-vortex}}^{\text{blowup-rate}}\sqrt{T_c - t},$$
   $$\kappa_{2D\text{-vortex}}^{\text{blowup-rate}} = \sqrt{2\cdot 1.384} \approx 1.664.$$

   In addition, there is an excellent match between the parameter $\kappa = \kappa_S(\sigma = 3) \approx 1.664$ of the admissible S profile, see (19), and the value of $\kappa_{2D\text{-vortex}}^{\text{blowup-rate}} \approx 1.664$ extracted from the blowup rate of the two-dimensional vortex solution.

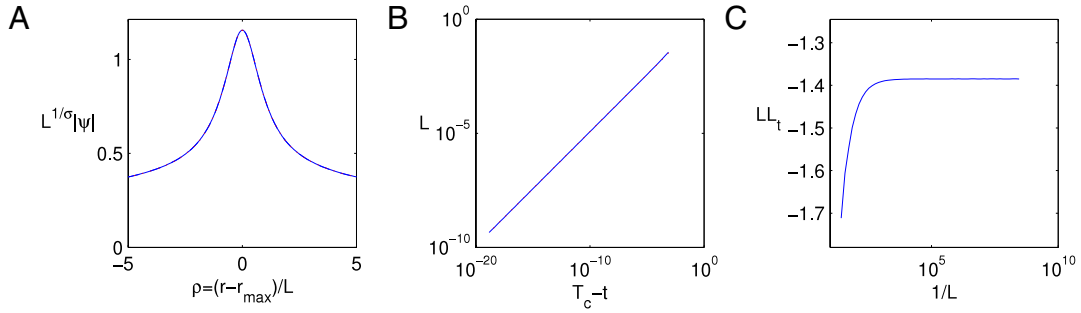

Fig. 15. Solution of Eq. (41) with $\sigma = 3$, $m = 1$, and the initial condition (43). (A) Rescaled solution according to (28) at focusing levels $1/L = 10^4$ (solid) and $1/L = 10^8$ (dashed), the dotted curve is the asymptotic profile S, and the dashed curve is the rescaled solution of the one-dimensional NLS at $1/L = 10^8$, taken from Fig. 7A. All four curves are indistinguishable. (B) L as a function of $(T_c - t)$ on a logarithmic scale. The dotted curve is the fitted curve $1.71(T_c - t)^{0.5007}$. The two curves are indistinguishable. (C) LL_t as a function of $1/L$.

6. Singular peak-type solutions of the one-dimensional supercritical BNLS

In Section 2 we reviewed the theory of singular peak-type solutions of the one-dimensional NLS. In this section, we present the analogous findings for the one-dimensional BNLS. We will make use of these results in the study of singular standing-ring solutions of the BNLS in Section 7.

6.1. Analysis

Let us consider the one-dimensional supercritical focusing BNLS

$$\mathrm{i}\phi_t(t,x) - \phi_{xxxx} + |\phi|^{2\sigma}\phi = 0, \quad \sigma > 4. \tag{44}$$

At present, there is no theory for singular peak-type solutions of Eq. (44). A recent numerical study [9] suggests that peak-type singular solutions of the supercritical BNLS (44) collapse with a self-similar asymptotic profile ϕ_B, i.e., $\phi \sim \phi_B$, where

$$\begin{aligned}\phi_B(t,x) &= \frac{1}{L^{2/\sigma}(t)}B(\xi)\mathrm{e}^{\mathrm{i}\tau}, \qquad \xi = \frac{x}{L(t)},\\ \tau(t) &= \int_{s=0}^{t}\frac{\mathrm{d}s}{L^4(s)}.\end{aligned} \tag{45}$$

The blowup rate $L(t)$ of these solutions is a quartic root, i.e.,

$$L(t) \sim \kappa_B\sqrt[4]{T_c - t}, \quad t \to T_c, \tag{46}$$

where $\kappa_B > 0$. In addition, the self-similar profile $B(\xi)$ is the solution of

$$B_{\xi\xi\xi\xi} - \frac{\mathrm{i}}{4}\kappa_B^4\xi B_\xi + \left(1 - \frac{\mathrm{i}}{2\sigma}\kappa_B^4\right)B(\xi) - |B|^{2\sigma}B = 0. \tag{47}$$

In general, symmetric solutions of (47) are complex-valued, and depend on the parameter κ_B and on the initial conditions $B(0)$ and $B''(0)$. We conjecture that, in analogy with the NLS, the following holds:

Conjecture 10. 1. *The nonlinear fourth-order ODE (47) has a unique 'admissible solution' with $\kappa_B = \kappa_B(\sigma)$, $B(0) = B_0(\sigma)$, $B''(0) = B_0''(\sigma)$ and a zero Hamiltonian.*
2. *This admissible solution is the self-similar profile of the asymptotic peak-type blowup profile ϕ_B, see (45).*
3. *The value of κ_B of the blowup rate (46) is equal to $\kappa_B(\sigma)$ of the admissible B profile.*

6.2. Simulations

We solve the one-dimensional BNLS (44) with $\sigma = 6$ and the Gaussian initial condition

$$\phi(t=0,x) = 1.6\cdot\mathrm{e}^{-x^2}. \tag{48}$$

We first show that the BNLS solution blows up with the self-similar profile ϕ_B, see (45). To do that, we rescale the solution according to

$$\phi_{\text{rescaled}}(t,x) = L^{2/\sigma}(t)\phi\left(\frac{x}{L(t)}\right), \quad L(t) = \|\phi\|_\infty^{-\sigma/2}. \tag{49}$$

The rescaled profiles at focusing levels of $1/L = 10^4$ and $1/L = 10^8$ are indistinguishable, see Fig. 16A, indicating that the solution is indeed self-similar while focusing over 4 orders of magnitude.

Next, we consider the blowup rate of the collapsing solution, see Fig. 16B. To do that, we first assume that

$$L(t) \sim \kappa_B(T_c - t)^p, \tag{50}$$

and find the best fitting κ_B and p. In this case $\kappa_B \approx 1.020$ and $p \approx 0.25017$, indicating that the blowup-rate is close to a quartic root. To verify that the blowup rate is indeed $p = 1/4$, we compute the limit $\lim_{t\to T_c} L^3L_t$. Note that for the quartic-root blowup rate (46)

$$\lim_{t\to T_c} L^3L_t = -\frac{\kappa_B^4}{4} < 0,$$

while for a faster-than-a-quartic root blowup rate $L^3L_t \to 0$. Since $\lim_{T_c\to t} L^3L_t \approx -0.2898$, see Fig. 16C, the blowup rate is a quartic-root (with no loglog correction), i.e.,

$$L(t) \sim \kappa_{B,1D}^{\text{blowup-rate}}\sqrt[4]{T_c - t}, \quad \kappa_{B,1D}^{\text{blowup-rate}} \approx \sqrt[4]{4\cdot 0.2898} \approx 1.0376.$$

7. Singular standing-ring solutions of the supercritical BNLS

In Section 3 we analyzed singular standing-ring solutions of the NLS with $\sigma > 2$. In this section, we derive the analogous results for the biharmonic NLS with $\sigma > 4$.

7.1. Analysis

Let us consider singular solutions of the focusing supercritical BNLS

$$\mathrm{i}\psi_t(t,r) - \Delta_r^2\psi + |\psi|^{2\sigma}\psi = 0, \quad \sigma d > 4,\ d > 1, \tag{51}$$

where

$$\begin{aligned}\Delta_r^2 = &-\frac{(d-1)(d-3)}{r^3}\partial_r + \frac{(d-1)(d-3)}{r^2}\partial_r^2\\ &+ \frac{2(d-1)}{r}\partial_r^3 + \partial_r^4\end{aligned} \tag{52}$$

is the radial biharmonic operator. The following lemma, which is the BNLS analogue of Lemma 1, shows that standing-ring collapse can only occur for $\sigma \geq 4$:

Lemma 11. *Let ψ be a self-similar standing-ring singular solution of the BNLS (10), i.e., $\psi \sim \psi_B$, where*

$$|\psi_B(t,r)| = \frac{1}{L^{2/\sigma}(t)}|B(\rho)|, \quad \rho = \frac{r - r_{\max}(t)}{L(t)}, \tag{53a}$$

and

$$0 < \lim_{t\to T_c} r_{\max}(t) < \infty. \tag{53b}$$

Then, $\sigma \geq 4$.

Proof. Integration gives $\|\psi_B\|_2^2 = \mathcal{O}\left(L^{1-4/\sigma}\right)$, and so the proof of Lemma 1 holds for $\sigma \geq 4$. □

Corollary 12. *ψ_B undergoes a strong collapse when $\sigma = 4$, and a weak collapse when $\sigma > 4$.*

Proof. This follows directly from the proof of Lemma 11. □

Let us further consider standing-ring solutions of the BNLS (51). In this case, in the ring region of a standing ring solution, the terms of the biharmonic operator, see (52), behave as

$$\left[\frac{1}{r^{4-k}}\partial_r^k\psi\right] = \mathcal{O}\left(L^{-k}\right), \quad k = 0,\ldots,4.$$

Therefore, $\Delta_r^2\psi \sim \partial_r^4\psi$. Hence, near the singularity, Eq. (51) reduces to the one-dimensional BNLS (44), i.e.,

$$\psi(t,r) \sim \phi\left(t, x = r - r_{\max}(t)\right), \tag{54}$$

where ϕ is a peak-type solution of the one-dimensional BNLS (44). Therefore, we predicted in [11] and also confirmed numerically that the blowup dynamics of standing ring solutions of the NLS (51) with $d > 1$ and $\sigma = 4$ is the same as the blowup dynamics of singular peak solutions of the one-dimensional BNLS (51) with $\sigma = 4$. Similarly, we now predict that the blowup dynamics of standing ring solutions of the BNLS (51) with $d > 1$ and $\sigma > 4$ is the same as the blowup dynamics of collapsing peak solutions of the one-dimensional BNLS (44) with the same nonlinearity exponent σ:

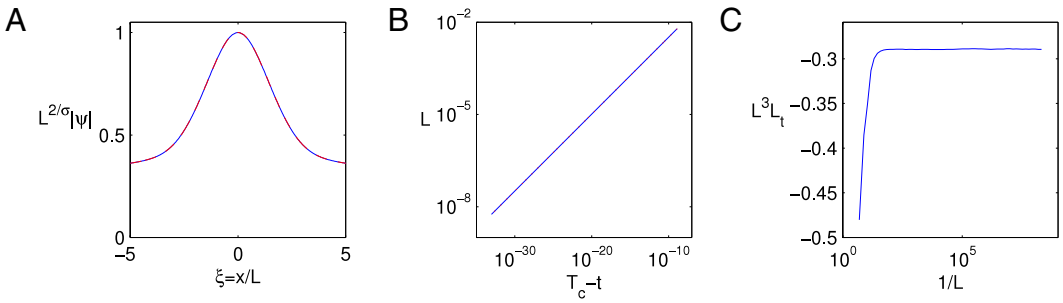

Fig. 16. Solution of the one-dimensional BNLS (44) with $\sigma = 6$ and the Gaussian initial condition (48). (A) Rescaled solution according to (49) at focusing levels $1/L = 10^4$ (solid) and $1/L = 10^8$ (dashed). The two curves are indistinguishable. (B) L as a function of $(T_c - t)$ on a logarithmic scale. The dotted curve is the fitted curve $1.020(T_c - t)^{0.25017}$. (C) $L^3 L_t$ as a function of $1/L$.

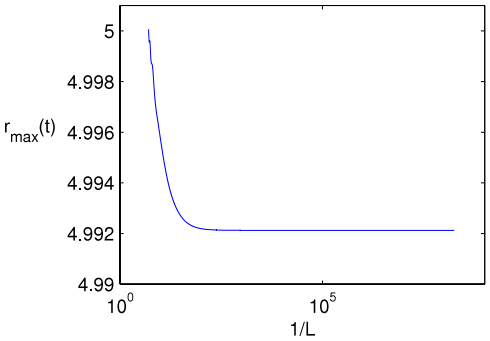

Fig. 17. Ring radius $r_{\max}(t)$ as a function of the focusing level $1/L(t)$ for the solution of the BNLS (10) with $d = 2$, $\sigma = 6$ and the initial condition $\psi_0(r) = 1.6 \cdot \mathrm{e}^{-(r-5)^2}$.

Conjecture 13. *Let ψ be a singular standing-ring solution of the BNLS (51) with $d > 1$ and $\sigma > 4$. Then,*

1. *The solution is self-similar in the ring region, i.e., $\psi \sim \psi_B$ for $r - r_{\max} = \mathcal{O}(L)$, where $|\psi_B|$ is given by (53a).*
2. *The self-similar profile ψ_B is given by*

$$\psi_B(t, r) = \phi_B\left(t, x = r - r_{\max}(t)\right), \tag{55}$$

where $\phi_B(t, x)$, see (45), is the asymptotic profile of the one-dimensional BNLS (44) with the same σ.

3. *The blowup rate is a quartic root, i.e.,*

$$L(t) \sim \kappa_B(\sigma)\sqrt[4]{T_c - t}, \quad t \to T_c, \tag{56}$$

where $\kappa_B(\sigma) > 0$ is the value of κ_B of the admissible B profile.

Conjecture 13 implies, in particular, that the parameter κ_B of the blowup-rate of ψ, see (56), is the same as the parameter κ_B of the blowup rate of ϕ, see (46). This value depends on the nonlinearity exponent σ, but is independent of the dimension d and of the initial condition ψ_0.

7.2. Simulations

We solve the BNLS (51) with $d = 2$ and $\sigma = 6$ with the initial condition $\psi_0(r) = 1.6 \cdot \mathrm{e}^{-(r-5)^2}$. In Fig. 17 we plot the ring radius $r_{\max}(t)$ as a function of the focusing factor $1/L(t)$, as the solution blows up over 8 orders of magnitude. Since $\lim_{t \to T_c} r_{\max}(t) = 4.992$, the ring is standing and is not shrinking or expanding. Note that the initial condition is different from the asymptotic profile ψ_B, suggesting that *standing-ring collapse is (radially) stable*.

We next test each item of Conjecture 13 numerically:

1. In Fig. 18A, we plot the rescaled solution

$$\psi_{\text{rescaled}} = L^{2/\sigma}(t)\psi\left(\frac{r - r_{\max}(t)}{L(t)}\right),$$
$$L(t) = \|\psi\|_\infty^{-\sigma/2}, \; r_{\max}(t) = \arg\max_r |\psi|, \tag{57}$$

at $1/L = 10^4$ and $1/L = 10^8$. The two curves are indistinguishable, showing that standing rings undergo a self-similar collapse with the self-similar ψ_B profile (45).

2. To verify that the self-similar collapse profile ψ_B is, up to a shift in r, equal to the asymptotic collapse profile ϕ_B of the one-dimensional BNLS (44), we superimpose the rescaled solution of the one-dimensional BNLS (44) from Fig. 16A, on to the rescaled solutions of Fig. 18A, and observe that, indeed, the curves are indistinguishable.
3. Fig. 18B shows that

$$L(t) \sim 1.020(T_c - t)^{0.25017}.$$

Therefore, the blowup rate is quartic root or slightly faster. Fig. 18C shows that $\lim_{T_c \to t} L^3 L_t \approx -0.2894$, indicating that the blowup rate is quartic-root (with no loglog correction), i.e.,

$$L(t) \sim \kappa_{B,2D}^{\text{blowup-rate}} \sqrt[4]{T_c - t},$$
$$\kappa_{B,2D}^{\text{blowup-rate}} \approx \sqrt[4]{4 \cdot 0.2894} \approx 1.0373.$$

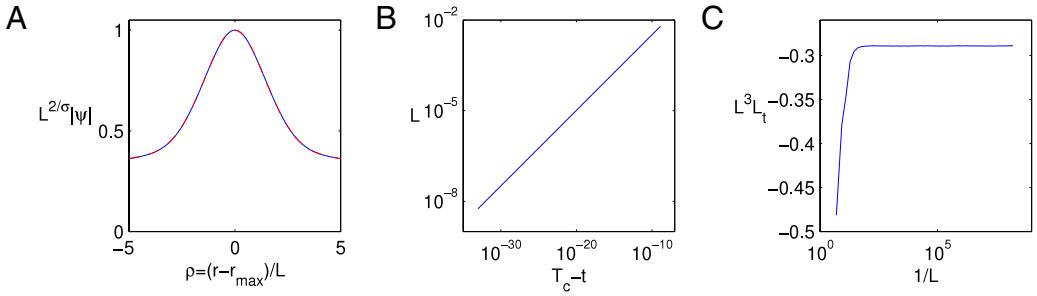

Fig. 18. Solution of the two-dimensional BNLS (10) with $\sigma = 6$ and the initial condition $\psi_0(x) = 1.6 \cdot \mathrm{e}^{-(r-5)^2}$. (A) Rescaled solution according to (49) at focusing levels $1/L = 10^4$ (solid) and $1/L = 10^8$ (dashed). The dashed curve is the rescaled solution of the one-dimensional BNLS at $1/L = 10^8$, taken from Fig. 16. All three curves are indistinguishable. (B) L as a function of $(T_c - t)$ on a logarithmic scale. The dotted curve is the fitted curve $1.020(T_c - t)^{0.2502}$. The two curves are indistinguishable. (C) $L^3 L_t$ as a function of $1/L$.

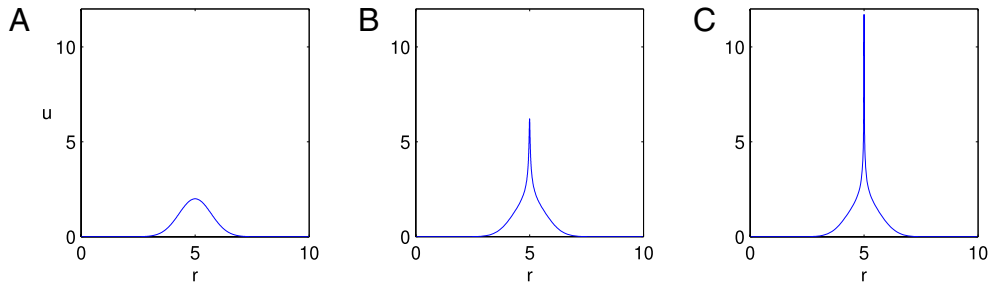

Fig. 19. Solution of the NLHE (58) with $d = 2$, $\sigma = 3$ and the initial condition (62). (A) $t = 0$. (B) $t = 0.002683$. (C) $t = 0.002686$.

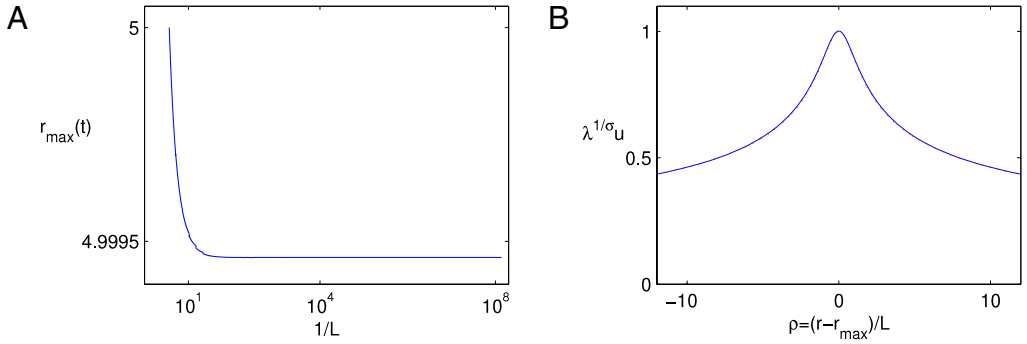

Fig. 20. Solution of Fig. 19. (A) Ring radius $r_{\max}(t)$ as a function of $1/L(t)$. (B) Solution u at $1/L = 10^8$ (solid curve). Dashed curve is the asymptotic u_S profile (64). Both curves are rescaled according to (63). The two curves are indistinguishable.

As predicted, there is an excellent match between the value of $\kappa_{B,2D}^{\text{blowup-rate}} \approx 1.0373$ extracted from the two-dimensional BNLS solution, and the value of $\kappa_{B,1D}^{\text{blowup-rate}} \approx 1.0376$ extracted from the one-dimensional BNLS solution, see Section 6.2.

8. Singular standing-ring solutions of the nonlinear heat equation

We now consider the d-dimensional radially-symmetric nonlinear heat equation (NLHE)

$$u_t(t,r) - \Delta u - |u|^{2\sigma}u = 0, \quad \sigma > 0,\ d > 1, \tag{58}$$

where u is real and $\Delta = \partial_{rr} + \frac{d-1}{r}\partial_r$. The existence of singular standing ring solutions of (58) was proved by Giga and Kohn [13]. We now study the relation between these solutions, and peak-type solutions of the one-dimensional NLHE.[2]

$$v_t(t,x) - v_{xx} - |v|^{2\sigma}v = 0, \quad \sigma > 0. \tag{59}$$

Eq. (59) admits singular solutions that collapse with the self-similar peak-type profile [24–26]

$$v_S(t,x) = \frac{1}{\lambda^{\frac{1}{\sigma}}(t)}\frac{1}{\left(1+\xi^2\right)^{\frac{1}{2\sigma}}}, \quad \xi = \frac{x}{L(t)}, \tag{60a}$$

where

$$\lambda(t) = \sqrt{2\sigma(T_c - t)},$$
$$L(t) = \sqrt{2\left(2 + \frac{1}{\sigma}\right)(T_c - t)\,|\ln(T_c - t)|}. \tag{60b}$$

Note that unlike the one-dimensional NLS, the one-dimensional NLHE admits singular solutions for any $\sigma > 0$.

[2] Throughout this paper, we denote the solution of the one-dimensional NLHE by v, and its spatial variable by x.

Let us consider singular standing-ring solutions of the NLHE (58). Since $\Delta u \sim u_{rr}$ in the ring region, near the singularity Eq. (58) reduces to the one-dimensional NLHE (59). Therefore, this suggests that singular standing-ring solutions of the NLHE (58) exist for any $\sigma > 0$, and that the blowup profile and blowup rate of these solutions are the same as those of singular peak-type solutions of the one-dimensional NLHE with the same σ. Indeed, we have the following result:

Theorem 14. *Let $u(t,r)$ be a singular standing-ring solution of the NLHE (58). Then, the solution is self-similar in the ring region, i.e., $u \sim u_S$ for $r - r_{\max} = \mathcal{O}(L)$, where*

$$u_S(t,r) = v_S\left(t, x = r - r_{\max}(t)\right), \tag{61}$$

and v_S is given by Eq. (60).

Theorem 14 was rigorously proved by Matos [14]. Subsequently, Zaag [27–30] improved the results of Matos, and obtained bounds for the convergence rate to the self-similar profile.

8.1. Simulations

We solve the NLHE (58) with $d = 2$ and $\sigma = 3$ and the initial condition

$$u_0(r) = 2e^{-2(r-5)^2}. \tag{62}$$

The solution blows up with a ring profile, see Fig. 19. Since $\lim_{t\to T_c} r_{\max}(t) = 4.9994 > 0$, see Fig. 20A, the ring is standing.

In order to show that the solution blows up with the self-similar u_S profile (61), we rescale the solution according to

$$u_{\text{rescaled}}(t,r) = \lambda^{\frac{1}{\sigma}}(t)\,u\left(\frac{r - r_{\max}}{L(t)}\right), \tag{63}$$

where $\lambda(t)$ and $L(t)$ are given by (60b) and T_c is extracted from the numerical simulation. The rescaled profile at $1/L = 10^8$ is in perfect agreement with the rescaled u_S profile

$$u_{S,\text{rescaled}} = \frac{1}{\left(1+\rho^2\right)^{\frac{1}{2\sigma}}}, \tag{64}$$

see Fig. 20B.

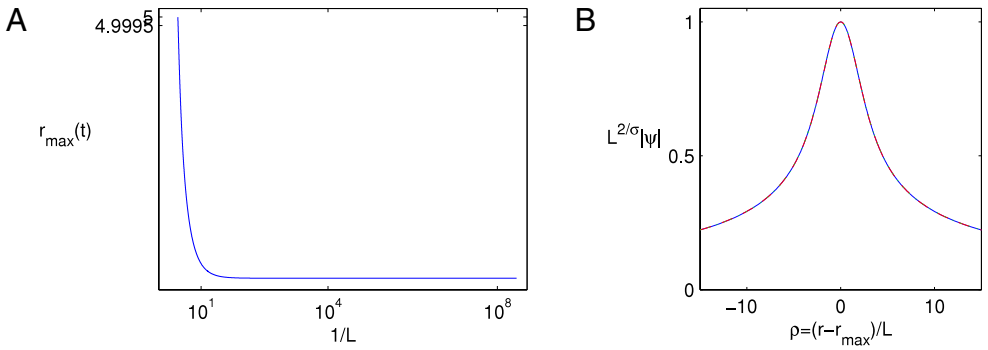

Fig. 21. Standing ring solution of the BNLHE (65) with initial condition (62). (A) ring radius $r_{\max}(t)$ as a function of $1/L(t)$ (B) solution u rescaled according to (57), at focusing factors of $1/L = 10^4$ (solid curve) and $1/L = 10^8$ (dashed curve). The rescaled peak-type solution of the one-dimensional NLH (66) is given by the dotted curve. All three curves are indistinguishable.

We note that Matos [14] showed that there is a different type of singular ring solutions, which is believed to be unstable (this has been proved in one dimension [25]). This is probably the reason why our numerical simulations only captured the ring solutions of Theorem 14.

9. Singular standing-ring solutions of the nonlinear biharmonic heat equation

The d-dimensional radially-symmetric biharmonic nonlinear heat (BNLHE) equation

$$u_t(t,r) + \Delta^2 u - |u|^{2\sigma}u = 0, \quad \sigma > 0,\ d > 1, \tag{65}$$

where u is real and Δ^2 is the radial biharmonic operator (52), admits singular solutions for any $\sigma > 0$ [15]. To the best of our knowledge, all known singular solutions of the BNLHE (65) collapse at a point. We now show that the BNLHE admits singular standing-ring solutions. The blowup profile and blowup rate of these solutions are the same as those of singular peak-type solutions of the one-dimensional BNLHE with the same σ.

9.1. Peak-type solutions of the one-dimensional BNLHE (review)

The one-dimensional BNLHE equation

$$v_t(t,x) + v_{xxxx} - |v|^{2\sigma}v = 0, \quad \sigma > 0, \tag{66}$$

admits singular peak-type solutions which collapse with the self-similar peak-type profile

$$v_B(t,x) = \frac{1}{L^{2/\sigma}(t)}B(\xi), \quad L(t) = \kappa_{\rm BH}\sqrt[4]{T_c - t},\ \xi = \frac{x}{L(t)}, \tag{67}$$

see [15]. The self-similar profile $B(\xi)$ is not known explicitly. Unlike the one-dimensional BNLS, the one-dimensional BNLHE admits singular solutions for any $\sigma > 0$.

9.2. Analysis

Let us consider singular standing-ring solutions of the BNLHE (65). Since $\Delta^2 u \sim u_{rrrr}$ in the ring region, near the singularity the BNLHE (65) reduces to the one-dimensional BNLHE (66). We therefore conjecture that standing-ring solutions of Eq. (65) exist, and that their blowup profile and blowup rate is the same as those of singular peak solutions of Eq. (66):

Conjecture 15. *Let $u(t,r)$ be a singular standing-ring solution of the BNLHE (65). Then, the solution is self-similar in the ring region, i.e., $u \sim u_B$ for $r - r_{\max} = \mathcal{O}(L)$, where*

$$u_B(t,r) = v_B\left(t, x = r - r_{\max}(t)\right), \tag{68}$$

and v_B is given by Eq. (67).

9.3. Simulations

We solve the BNLHE (65) with $d = 2$ and $\sigma = 3$ and the initial condition (62). The solution blows up with a standing-ring profile, see Fig. 21A. In Fig. 21B we plot the solution, rescaled according to (57), at focusing levels of $1/L = 10^4$ and $1/L = 10^8$. The two curves are indistinguishable, indicating that the solution is indeed self-similar. Next, we want to show that the self-similar blowup profile is given by $B(\xi)$, the self-similar profile of peak-type solutions of the one-dimensional NLHE, see (67). To do that, we compute the solution of the one-dimensional BNLHE (66) with $\sigma = 3$ and $u(t = 0, x) = 2e^{-x^2}$, and superimpose its profile at $1/L = 10^8$ in Fig. 21B. The three rescaled solutions are indistinguishable, indicating that standing-ring solutions of the BNLHE blowup with the self-similar profile of peak-type solutions of the one-dimensional BNLHE. In addition, we have from the numerical simulations that $\lim_{t\to T_c} L^3 L_t \approx -1.2108$ when $d = 2$, where $L(t) := \|u\|_\infty^{-\sigma/2}$, and $\lim_{t\to T_c} L^3 L_t \approx -1.2108$ when $d = 1$, where $L(t) := \|v\|_\infty^{-\sigma/2}$. Therefore, the blowup rate of the standing-ring solution of the two-dimensional BNLHE is equal, up to 5 significant digits, to the blowup rate of the singular peak-type solution of the one-dimensional BNLHE, and is given by

$$L(t) \sim \kappa_{\rm BH}\sqrt[4]{T_c - t}, \quad \kappa_{\rm BH} \approx \sqrt[4]{4 \cdot 1.2108} \approx 1.4835.$$

Thus, the numerical results provide a strong support for Conjecture 15.

10. Numerical methods

10.1. Admissible solutions of (17)

The admissible solution S of (17) was calculated using the shooting method of Budd et al. [31, Section 3.1]. In this method, one searches in the two-parameter space $(S(0), f_c)$ for the parameters such that the solution of (17) satisfies the admissible solution condition

$$\lim_{\xi\to\infty} F(\xi; f_c, S(0)) = 0,$$

$$F(\xi; f_c, S(0)) = \left|\xi S'(\xi) + \left(\frac{2\mathrm{i}}{f_c^2} + \frac{1}{\sigma}\right)S(\xi)\right|^2.$$

10.2. Solution of the NLS, BNLS, NLHE and BNLHE

In this study, we computed singular solutions of the NLS (4), the BNLS (51), the NLHE (58) and the BNLHE (65). These solutions become highly-localized, so that the spatial scale-difference between the singular region $r - r_{\max} = \mathcal{O}(L)$ and the exterior regions can be

as large as $\mathcal{O}(1/L) \sim 10^{10}$. In order to resolve the solution at both the singular and non-singular regions, we use an adaptive grid.

We generate the adaptive grids using the *Static Grid Redistribution* (SGR) method, which was first introduced by Ren and Wang [32], and was later simplified and improved by Gavish and Ditkowsky [33]. Using this approach, the solution is allowed to propagate (self-focus) until it starts to become under-resolved. At this stage, a new grid, with the same number of grid-points, is generated using De'Boors 'equidistribution principle', see [32,33] for details.

The method in [33] also allows control of the portion of grid points that migrate into the singular region, preventing under-resolution at the exterior regions. In [11], we further extended the approach to prevent under-resolution in the transition region $\mathcal{O}(L) \ll r - r_{\max} \ll O(1)$.

On the sequence of grids, the equations are solved using a Predictor–Corrector Crank–Nicholson scheme.

Acknowledgements

This research was partially supported by the Israel Science Foundation (ISF grant No. 123/08). The research of Nir Gavish was also partially supported by the Israel Ministry of Science Culture and Sports.

References

[1] P. Raphael, Existence and stability of a solution blowing up on a sphere for a L^2 supercritical nonlinear Schrödinger equation, Duke Math. J. 134 (2) (2006) 199–258.
[2] G. Fibich, N. Gavish, X.P. Wang, Singular ring solutions of critical and supercritical nonlinear Schrödinger equations, Physica D 231 (2007) 55–86.
[3] G. Fibich, N. Gavish, Theory of singular vortex solutions of the nonlinear Schrödinger equation, Physica D 237 (2008) 2696–2730.
[4] P. Raphael, J. Szeftel, Standing ring blow up solutions to the n-dimensional quintic nonlinear Schrödinger equation, Comm. Math. Phys. (2009) doi:10.1007/s00220-009-0796-2.
[5] F. Merle, P. Raphael, Sharp upper bound on the blow-up rate for the critical nonlinear Schrödinger equation, Geom. Funct. Anal. 13 (2003) 591–642.
[6] C. Sulem, P.L. Sulem, The Nonlinear Schrödinger Equation, Springer, New York, 1999.
[7] G. Fibich, N. Gavish, X.P. Wang, New singular solutions of the nonlinear Schrödinger equation, Physica D 211 (2005) 193–220.
[8] B. Ilan, G. Fibich, G. Papanicolaou, Self-focusing with fourth-order dispersion, SIAM J. Appl. Math. 62 (4) (2002) 1437–1462.
[9] G. Baruch, G. Fibich, E. Mandelbaum, Singular solutions of the biharmonic NLS, 2009. http://arxiv.org/abs/0912.1233.
[10] G. Baruch, G. Fibich, E. Mandelbaum, Singular solutions of the L^2-critical biharmonic nonlinear Schrödinger equation, Preprint, 2009.
[11] G. Baruch, G. Fibich, E. Mandelbaum, Ring-type singular solutions of the biharmonic nonlinear Schrödinger equation, Preprint, 2009.
[12] Y. Giga, R.V. Kohn, Asymptotically self-similar blow-up of semilinear heat equations, Comm. Adv. Pure Appl. Math. 38 (1985) 297–319.
[13] Y. Giga, R.V. Kohn, Nondegeneracy of blowup for semilinear heat equations, Comm. Pure Appl. Math. 42 (1989) 845–884.
[14] J. Matos, Unfocused blowup solutions of semilinear parabolic equations, Discrete Contin. Dyn. Syst. 5 (1999) 905–928.
[15] C.J. Budd, J.F. Williams, V.A. Galaktionov, Self-similar blow-up in higher-order semilinear parabolic equations, SIAM J. Appl. Math. 64 (5) (2004) 1775–1809.
[16] V.A. Galaktionov, J.L. Vazquez, Extinction for a quasilinear heat equation with absorprtion I. Technique of intersection comparison, Comm. Partial Differential Equations 19 (1994) 1075–1106.
[17] Victor A. Galaktionoy, Josephus Hulshof, Juan L. Vazquez, Extinction and focusing behaviour of spherical and annular flames described by a free boundary problem, J. Math. Pures Appl. 76 (7) (1997) 563–608.
[18] J.L. Velázquez, Singular solutions of partial differential equations modelling chemotactic aggregation, in: Proceedings of the International Congress of Mathematics, Madrid 2006, vol. III, 2006, pp. 321–338.
[19] M.A. Herrero, E. Medina, J.J.L. Velzquez, Finite-time aggregation into a single point in a reaction–diffusion system, Nonlinearity 10 (1997) 1739–1754.
[20] M.A. Herrero, E. Medina, J.J.L. Velzquez, Self-similar blow-up for a reaction–diffusion system, J. Comput. Appl. Math. 97 (1–2) (1998) 99–119.
[21] N. Gavish, G. Fibich, L.T. Vuong, A.L. Gaeta, Predicting the filamentation of high-power beams and pulses without numerical integration: a nonlinear geometrical optics method, Phys. Rev. A 78 (2008) 043807.
[22] T.D. Grow, A.A. Ishaaya, L.T. Vuong, A.L. Gaeta, N. Gavish, G. Fibich, Collapse dynamics of super-Gaussian beams, Opt. Express 14 (2006) 5468–5475.
[23] F. Merle, Limit of the solution of a nonlinear Schrödinger equation at blow-up time, J. Funct. Anal. 84 (1989) 201–214.
[24] J. Bricmont, A. Kupiainen, Universality in blowup for nonlinear heat equations, Nonlinearity 7 (1994) 539–575.
[25] M.A. Herrero, J.J.L. Velaquez, Blowup behavior of one-dimensional semilinear parabolic equations, Ann. Inst. H. Poincaré Anal. Non Linéaire 10 (1993) 131–189.
[26] J.J.L. Velaquez, Classification of singularities for blowing up solutions in higher dimensions, Trans. Amer. Math. Soc. 338 (1993) 441–464.
[27] H. Zaag, On the regularity of the blow-up set for semilinear heat equations, Ann. Inst. H. Poincaré Sect. B Probab. Statist. 19 (2002) 505–542.
[28] H. Zaag, One dimensional behavior of singular n dimensional solutions of semilinear heat equations, Comm. Math. Phys. 225 (2002) 523–549.
[29] H. Zaag, Regularity of blowup set and singular behaviour of semilinear heat equations, in: Mathematics and Mathematics Education, Bethlehem, 2000, vol. 225, 2002, pp. 337–344.
[30] H. Zaag, Determination of the curvature of the blowup set and refined singular behavior for semilinear heat equations, Duke Math. J. 133 (2006) 499–525.
[31] C.J. Budd, S. Chen, R.D. Russell, New self-similar solutions of the nonlinear Schrödinger equation with moving mesh computations, J. Comput. Phys. 152 (1999) 756–789.
[32] W. Ren, X.P. Wang, An iterative grid redistribution method for singular problems in multiple dimensions, J. Comput. Phys. 159 (2000) 246–273.
[33] A. Ditkowsky, N. Gavish, A grid redistribution method for singular problems, J. Comput. Phys. 228 (2009) 2354–2365.